

Computational Methods for the Analysis of Ascending Aortic Aneurysms

Antonio Martínez Pascual

Under the supervision of:

Prof. Marco Evangelos Biancolini

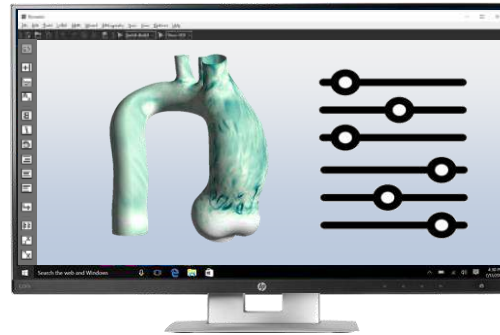
Michel Rochette Ph.D.



Overview



Pathology



Solution

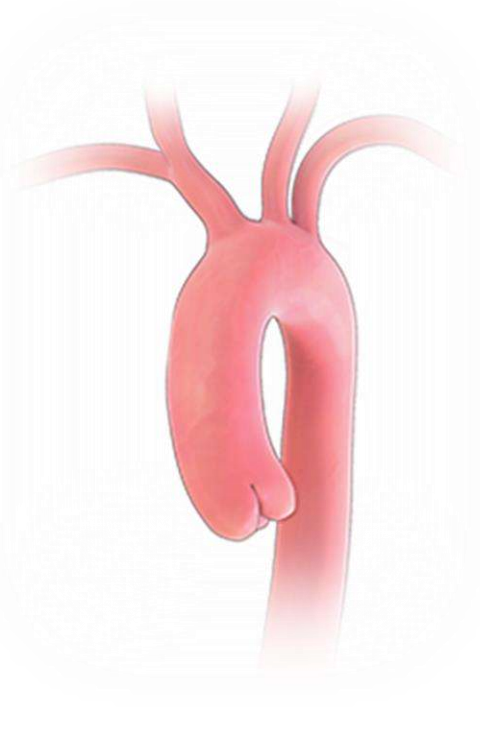
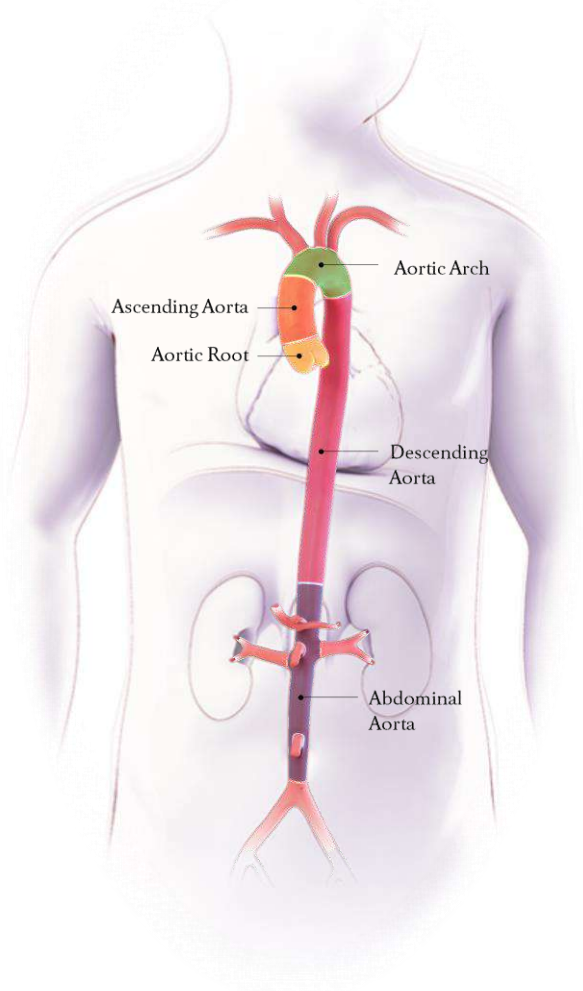


Outcome

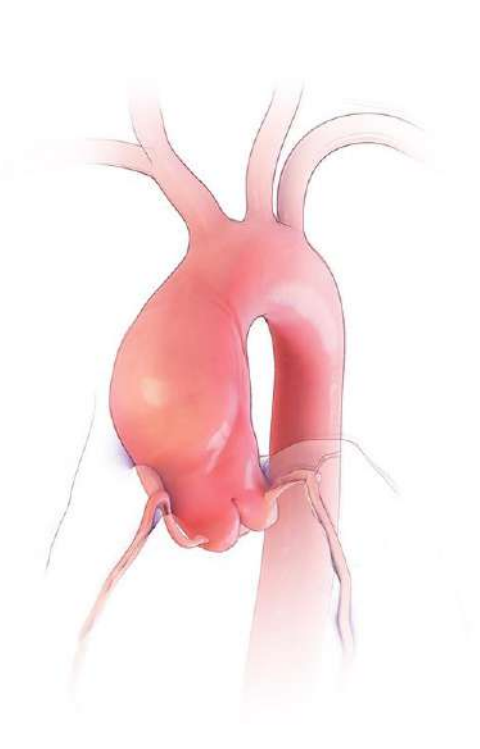
Introduction

A microscopic view of red blood cells (erythrocytes) in a blood smear. The cells are biconcave discs, appearing as reddish-orange discs with a lighter center. They are scattered across the field of view, with some in sharp focus and others blurred in the background. The background is a light, slightly hazy pinkish-white color.

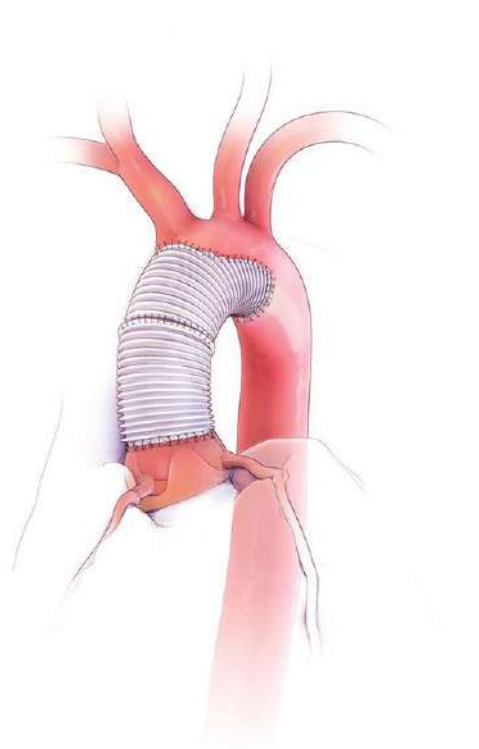
Aortic Aneurysms



Healthy



Aneurysm



Repaired

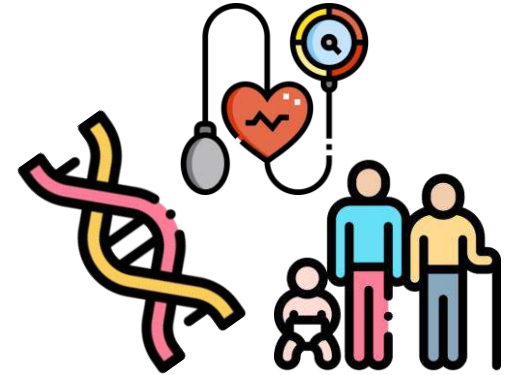
Aortic Aneurysms



5-10 cases per
100,000 person/year

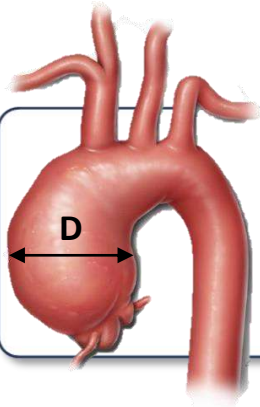


22% of patients with ruptured
aneurysm die before reaching
a hospital

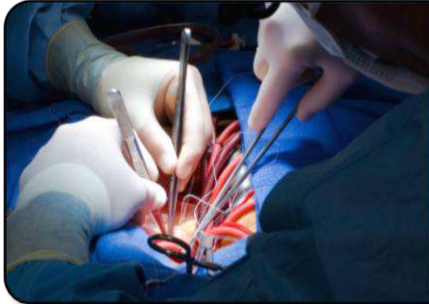


Linked to age, sex, hypertension,
genetic conditions

Clinical problem



Current practice:
Surgery is determined by **diameter**.



Problem:

- ▶ It's too generic
- ▶ Unpredicted aneurysm rupture
- ▶ Unnecessary intervention

Post-operative complications:

- ▶ Hemorrhage
- ▶ Infection
- ▶ Cardiac fatigue.

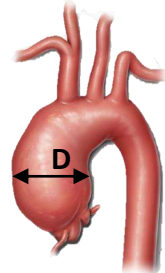


Clinical need to gain insight of the patient's
HEMODYNAMICS & WALL DETERIORATION
for accurate personalized treatment

Surgical decision



Data acquisition



Measurement



Medication

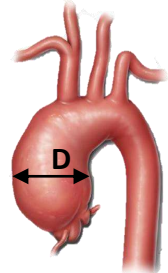


Surgery

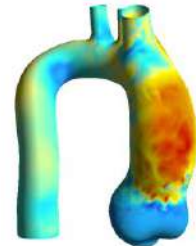
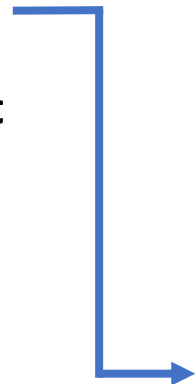
Surgical decision



Data acquisition



Measurement



Computational Biomarkers



Medication



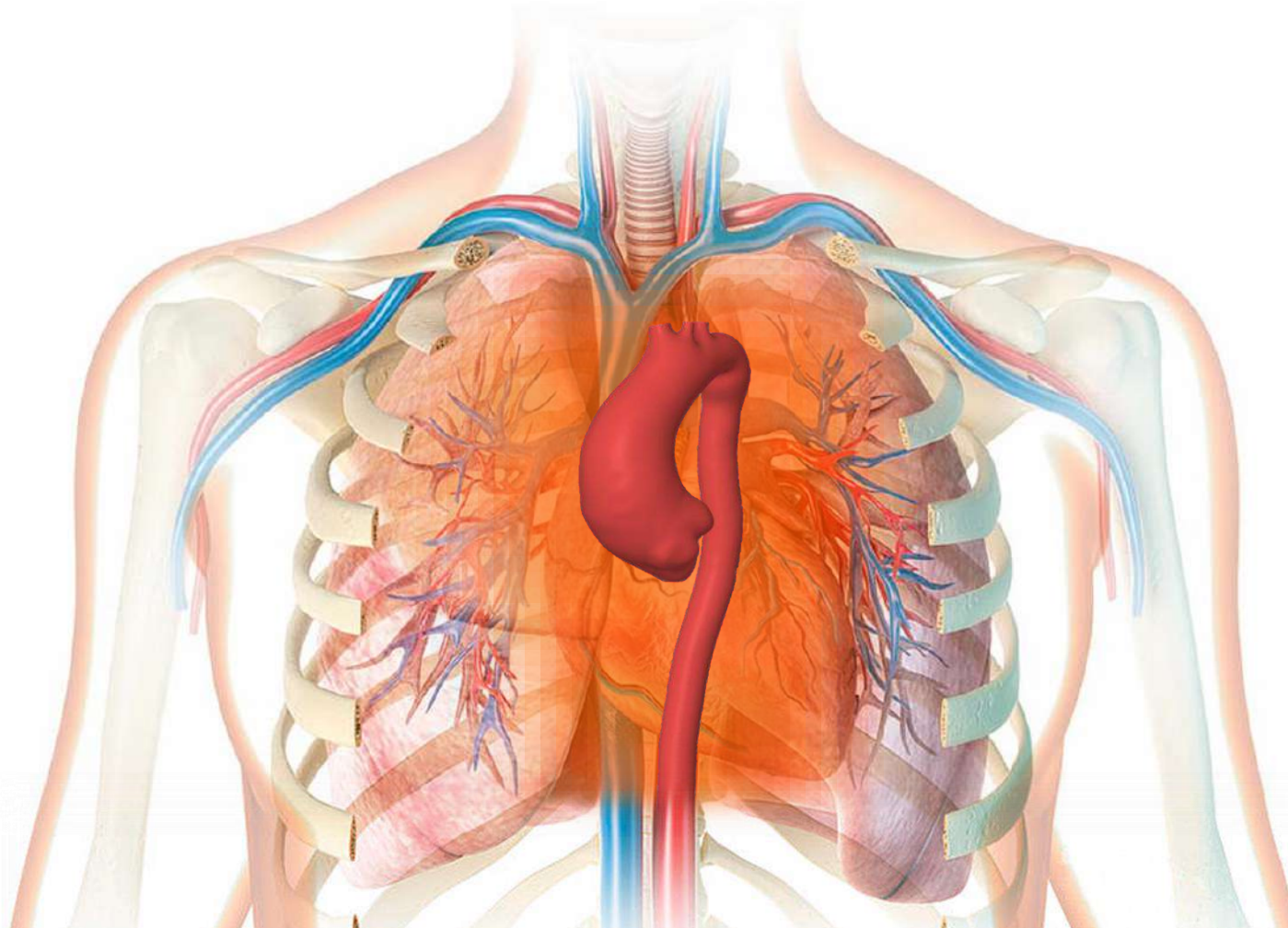
Surgery

Patient specific diagnosis

Aortic Aneurysm

Patient specific:

- ▶ Aorta Shape
- ▶ Valve morphology
- ▶ Valve pathology
- ▶ Hemodynamic BCs
- ▶ Aortic wall

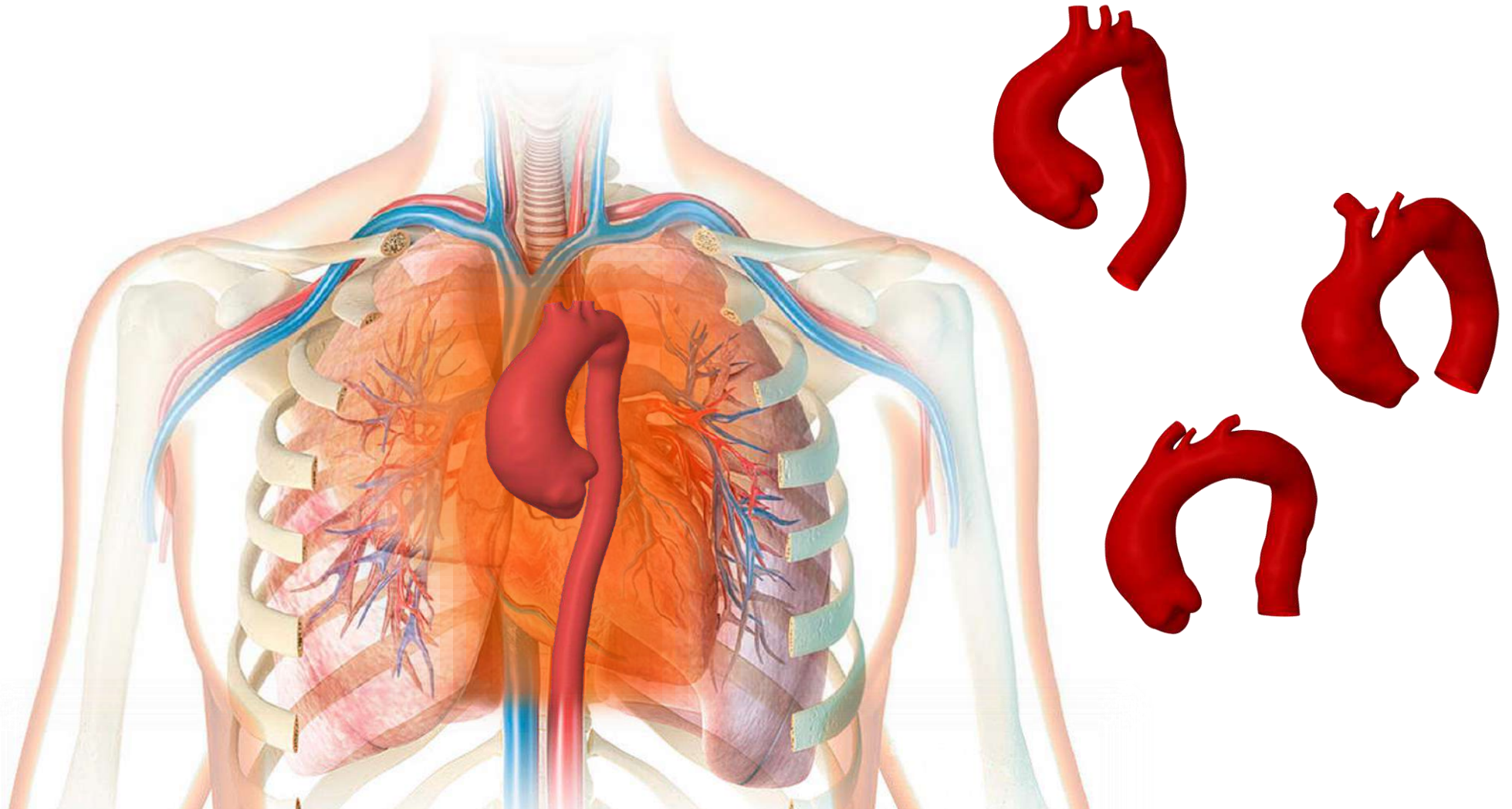


Patient specific diagnosis

Aortic Aneurysm

Patient specific:

- ▶ Aorta Shape
- ▶ Valve morphology
- ▶ Valve pathology
- ▶ Hemodynamic BCs
- ▶ Aortic wall

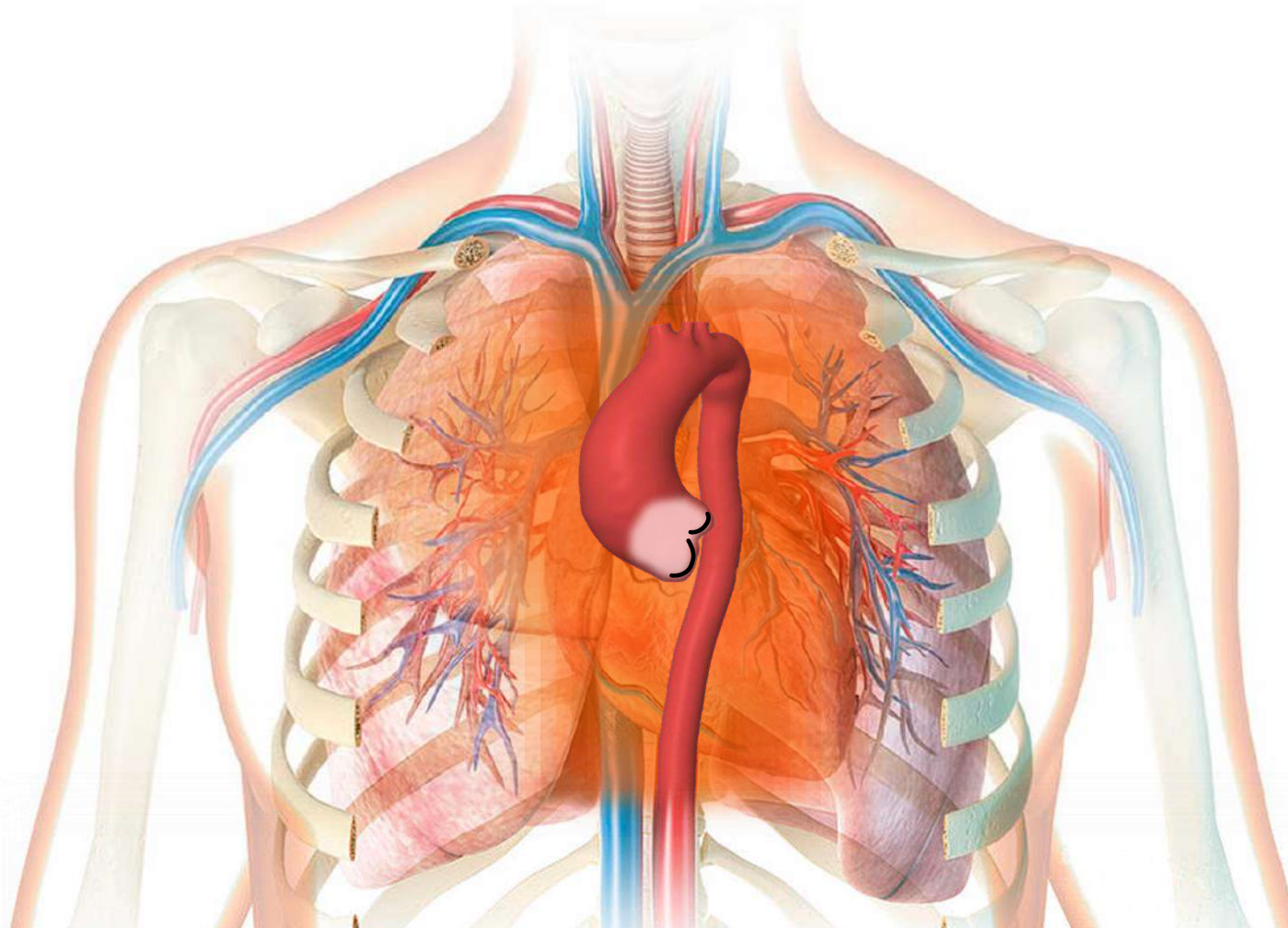


Patient specific diagnosis

Aortic Aneurysm

Patient specific:

- ▶ Aorta Shape
- ▶ Valve morphology
- ▶ Valve pathology
- ▶ Hemodynamic BCs
- ▶ Aortic wall

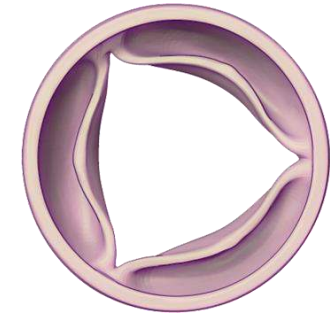
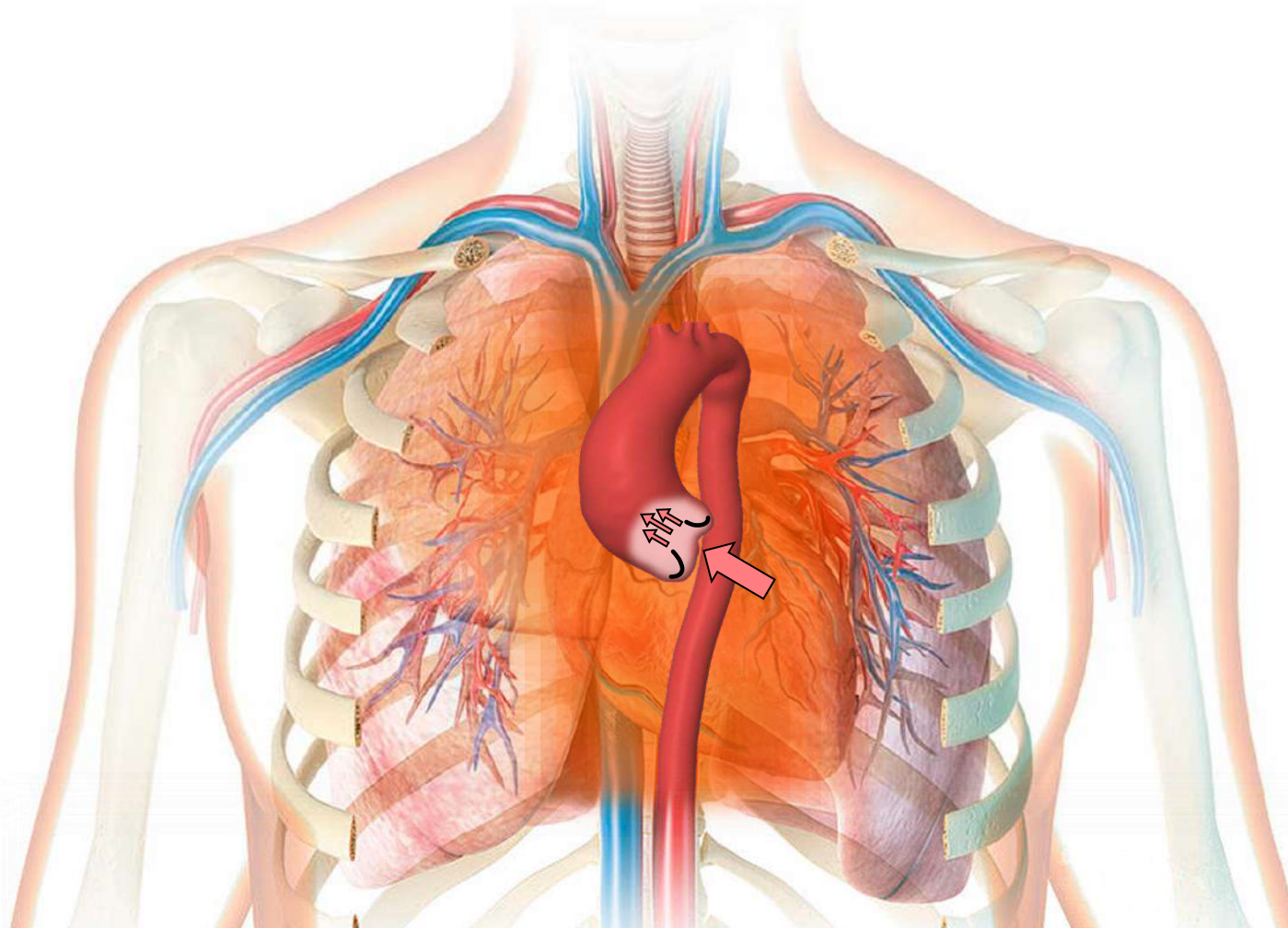


Patient specific diagnosis

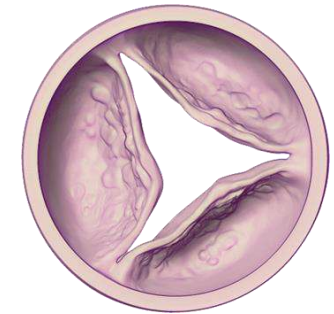
Aortic Aneurysm

Patient specific:

- ▶ Aorta Shape
- ▶ Valve morphology
- ▶ Valve pathology
- ▶ Hemodynamic BCs
- ▶ Aortic wall



Healthy



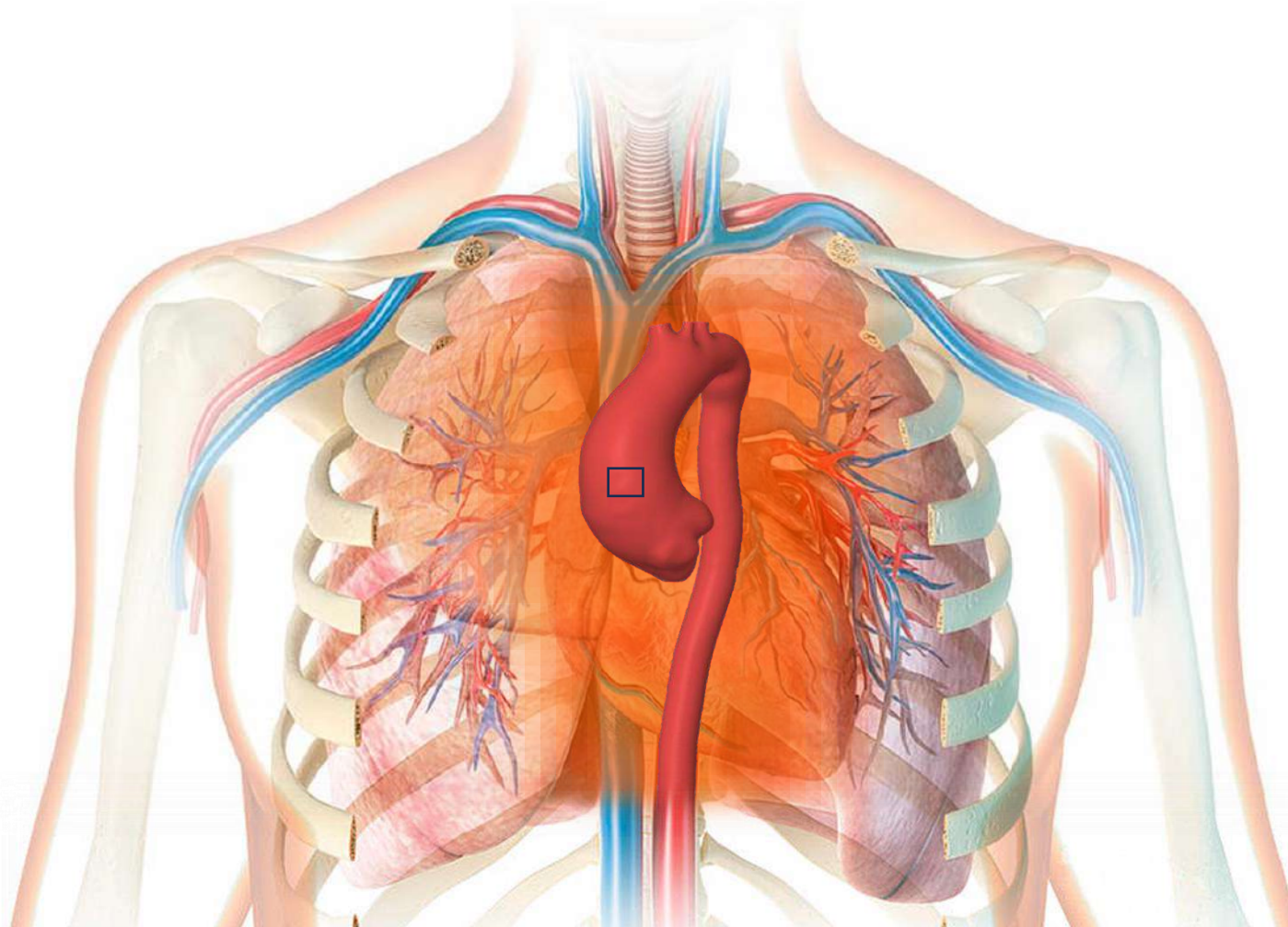
**Diseased
(Stenosis)**

Patient specific diagnosis

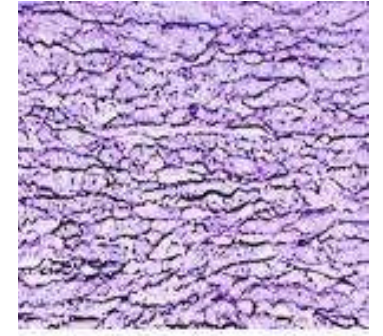
Aortic Aneurysm

Patient specific:

- ▶ Aorta Shape
- ▶ Valve morphology
- ▶ Valve pathology
- ▶ Hemodynamic BCs
- ▶ Aortic wall



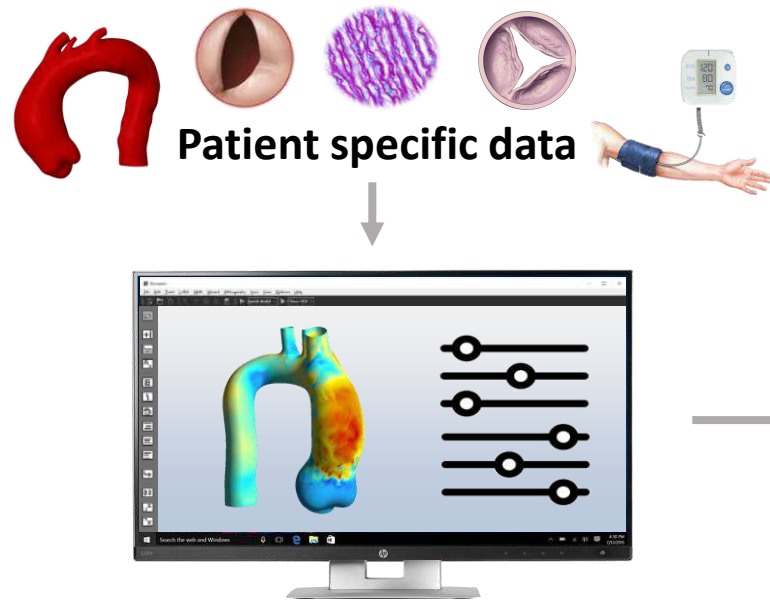
Healthy



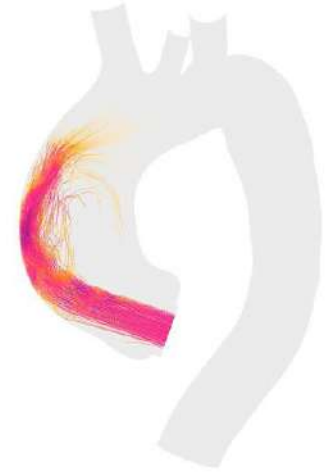
Aneurysm



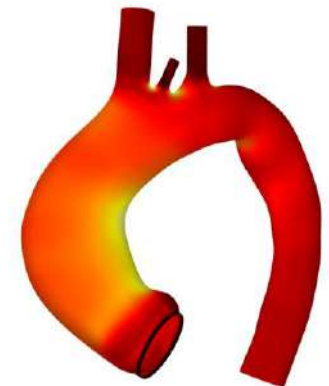
Computational tools for personalized treatment



Fluid biomarkers
WSS, Flow



Structural biomarkers
Stress



Section I

Computational methods for accurate turbulence and viscosity modelling

Introduction

No standardized methodology exists for the computation of cardiovascular flows



CFD results are influence by the modeling set-up



OBJECTIVE

Quantify the effect of model choices CFD results

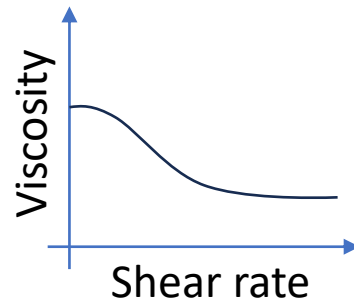
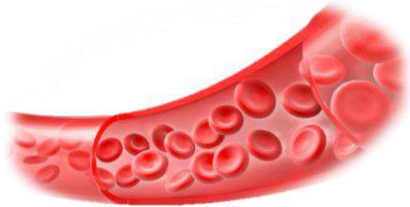
▶ **Viscosity**

▶ **Turbulence**

Introduction

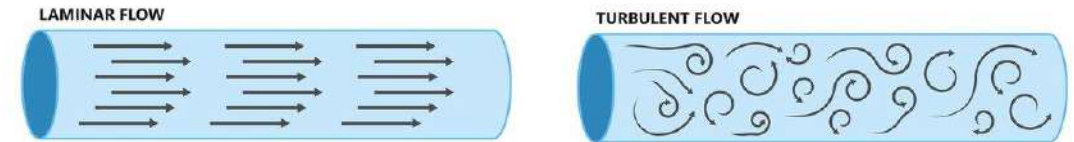
Viscosity

- ▶ Blood is a mixture of plasma and red blood cells with a shear-thinning behaviour.
- ▶ Eddy development and near-wall flow is influenced by this property [1].
- ▶ It is argued that, under the high shear-rates present in the aorta, the variations in viscosity are negligible and constant viscosity can be assumed.



Turbulence

- ▶ Turbulence causes bursts of shear stress, damaging endothelial cells [2].
- ▶ Turbulence generates additional stresses on aneurysm wall leading to wall vibration and increases the rate of wall dilation [2].
- ▶ Pulsatile flow with a low averaged Reynolds number, averaged Reynolds suggests laminar flow.
- ▶ Flow deceleration during diastole favours turbulence generation.



[1] Wyk et al., "Non-Newtonian perspectives on pulsatile blood-analog flows in a 180° curved artery model", *Physics of Fluids* 27 (2015)

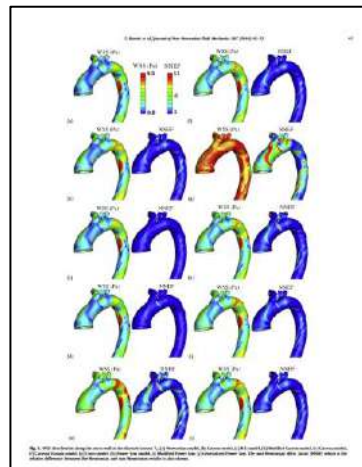
[2] Tan et al. "Analysis of flow patterns in a patient-specific thoracic aortic aneurysm model," *Computers and Structures* 87 (2009)

Previous work

Viscosity

Newtonian model causes:

- ▶ Underestimation of WSS and hemolysis
- ▶ Growth and decay of eddies
- ▶ Premature turbulent transition

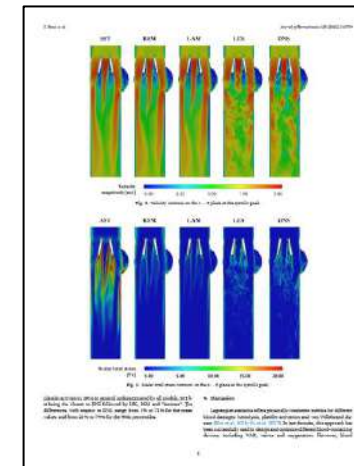


Karimi et al. *Journal of Non-Newtonian Fluid Mechanics* 207 (2014)

Turbulence

Laminar model causes:

- ▶ WSS underestimated between 0-6% (depending on author)
- ▶ Platelet activation and hemolysis
- ▶ Underestimated TKE



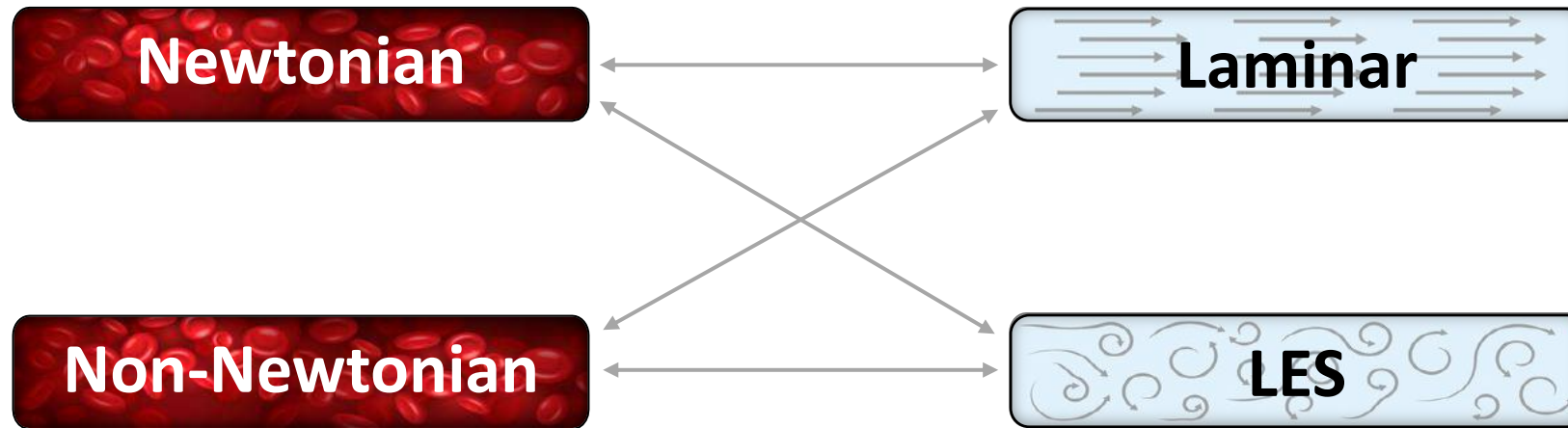
Bozzi et al. *Journal of Biomechanics* 128 (2021)

No publication exists on the combined effect of viscosity and turbulence models

Objective

Viscosity

Turbulence



Understand the interaction between models
and
the importance of the model choices

Scope

Viscosity

- ▶ **Newtonian:** $\mu(\dot{\gamma}) = \mu_{\infty}$
- ▶ **Non-Newtonian: Carreau viscosity (CV)**

$$\mu(\dot{\gamma}) = \mu_{\infty} + (\mu_0 - \mu_{\infty}) [1 + (\lambda\dot{\gamma})^2]^{\frac{n-1}{2}}$$

$$\mu_{\infty} = 3.5 \text{ mPa}\cdot\text{s}$$

$$\mu_0 = 56 \text{ mPa}\cdot\text{s}$$

$$\lambda = 3.313 \text{ s}$$

$$n = 0.3568$$

Turbulence

- ▶ **No model: Laminar flow model (LFM)**
- ▶ **Turbulent: LES**

$$\frac{\partial \bar{u}_i}{\partial x_i} = 0,$$

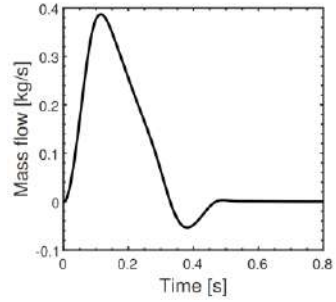
$$\frac{\partial \bar{u}_i}{\partial t} + \bar{u}_j \frac{\partial \bar{u}_i}{\partial x_j} = -\frac{1}{\rho} \frac{\partial \bar{p}}{\partial x_i} + \nu \frac{\partial}{\partial x_j} \left(\frac{\partial \bar{u}_i}{\partial x_j} \right) - \frac{\partial \tau_{ij}}{\partial x_j}$$

$$\tau_{ij} - \frac{1}{3} \tau_{kk} \delta_{ij} = -2\nu_{sgs} \bar{S}_{ij}$$

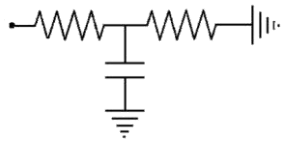
$$\nu_{sgs} = (C_S \Delta)^2 |\bar{S}|$$

Dynamic Smagorinsky-Lilly (DSL)
subgrid-scale turbulence model

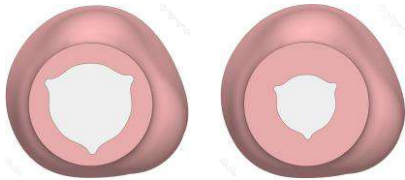
Model setup



Mass flow inlet



Windkessel outlets



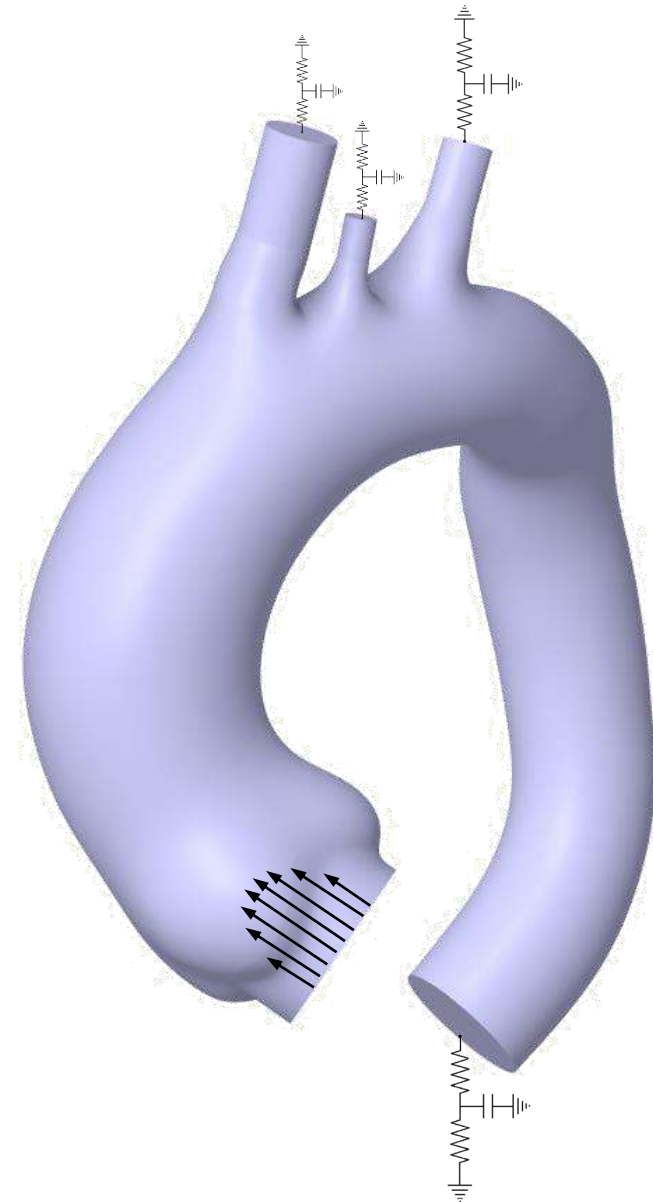
Aortic valve

- ▶ Healthy
- ▶ Stenotic



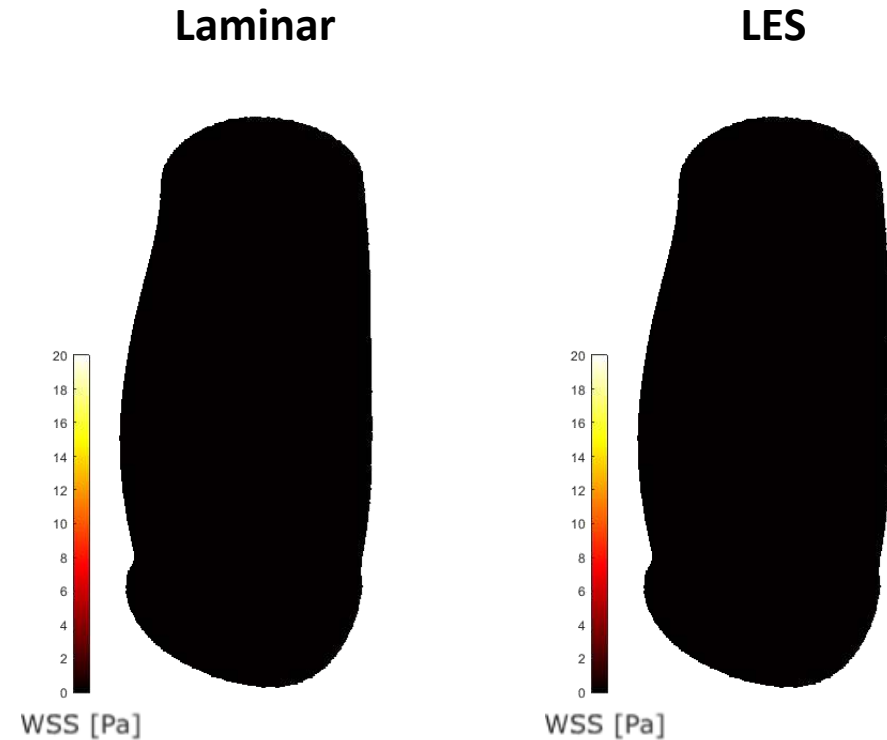
10 days per scenario

- ▶ 20 heart beats
- ▶ 32 cores



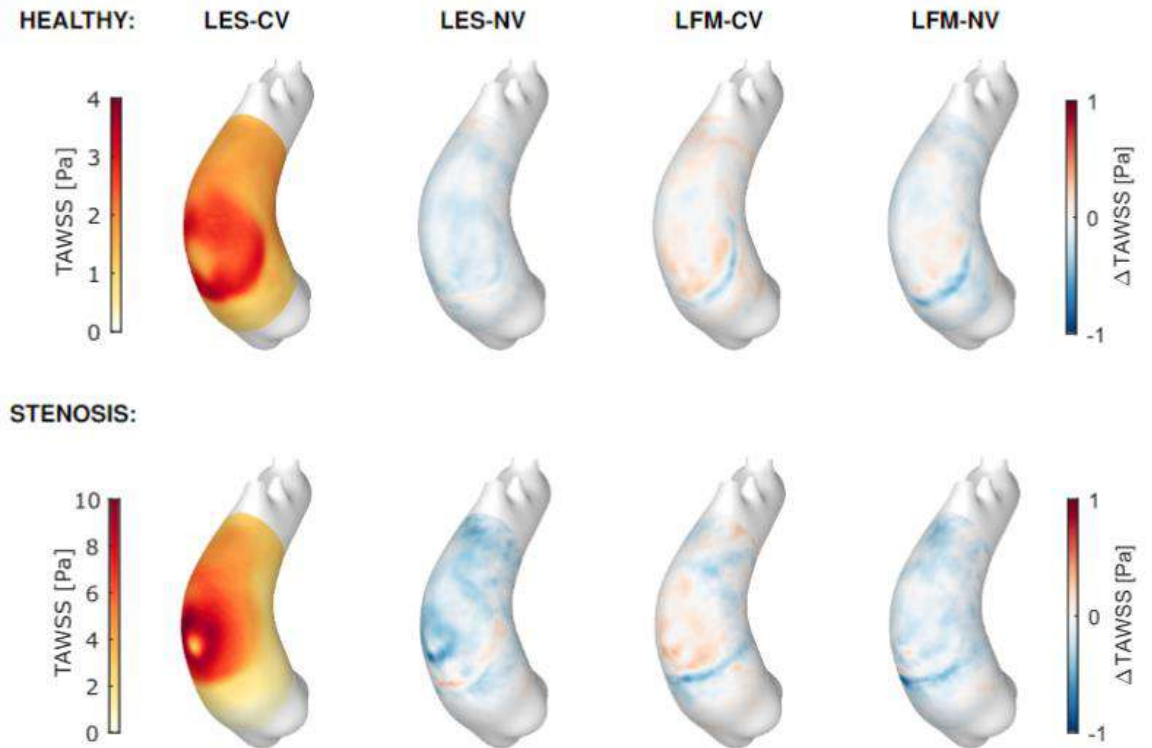
Results

- ▶ Vortex structure is influenced by the turbulence model.
- ▶ Non-Newtonian viscosity has greater impact (2.9-5.0%) on wall shear stress than Large Eddy Simulation turbulence modelling (0.1-1.4%).
- ▶ Wall shear stress is underestimated when considering Newtonian viscosity by 2.9-5.0%.
- ▶ The contribution of non-Newtonian viscosity is amplified when combined with a LES model.
- ▶ Cycle-to-cycle variability can impact the results as much as the numerical model if insufficient cycles are performed.



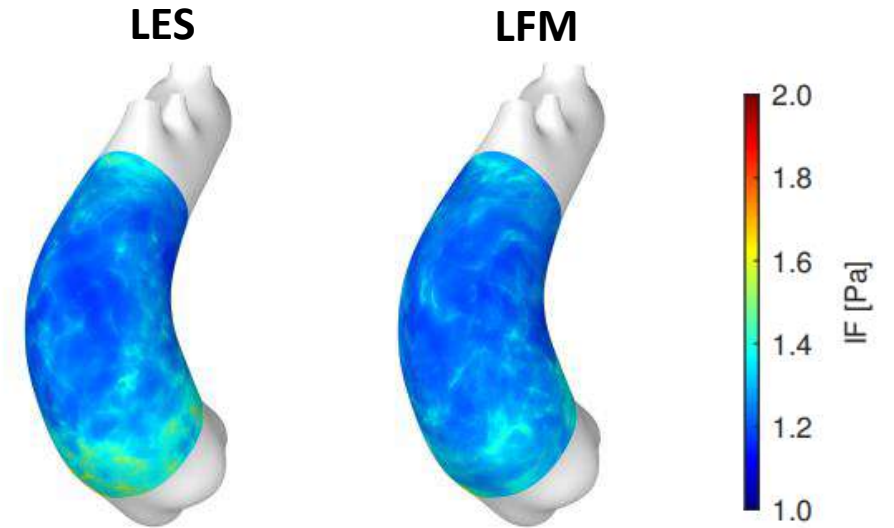
Results

- ▶ Vortex structure is influenced by the turbulence model.
- ▶ Non-Newtonian viscosity has greater impact (2.9-5.0%) on wall shear stress than Large Eddy Simulation turbulence modelling (0.1-1.4%).
- ▶ Wall shear stress is underestimated when considering Newtonian viscosity by 2.9-5.0%.
- ▶ The contribution of non-Newtonian viscosity is amplified when combined with a LES model.
- ▶ Cycle-to-cycle variability can impact the results as much as the numerical model if insufficient cycles are performed.



Results

- ▶ Vortex structure is influenced by the turbulence model.
- ▶ Non-Newtonian viscosity has greater impact (2.9-5.0%) on wall shear stress than Large Eddy Simulation turbulence modelling (0.1-1.4%).
- ▶ Wall shear stress is underestimated when considering Newtonian viscosity by 2.9-5.0%.
- ▶ The contribution of non-Newtonian viscosity is amplified when combined with a LES model.
- ▶ Cycle-to-cycle variability can impact the results as much as the numerical model if insufficient cycles are performed.

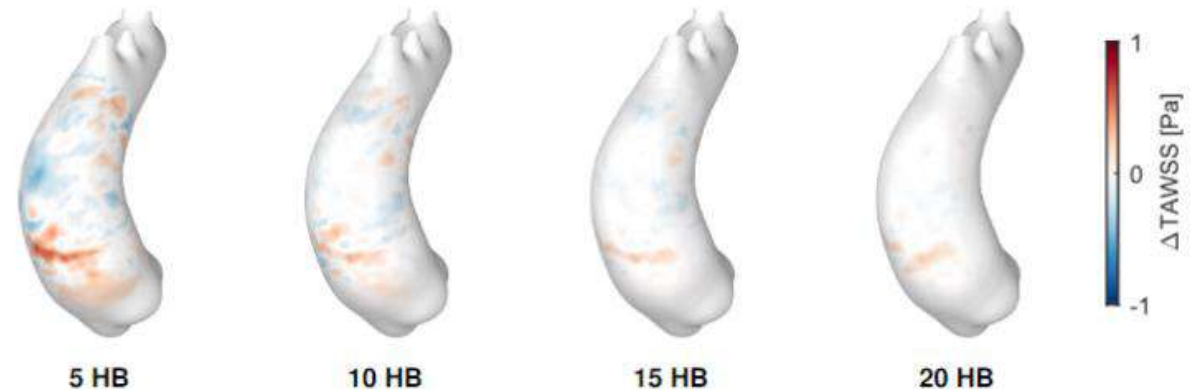
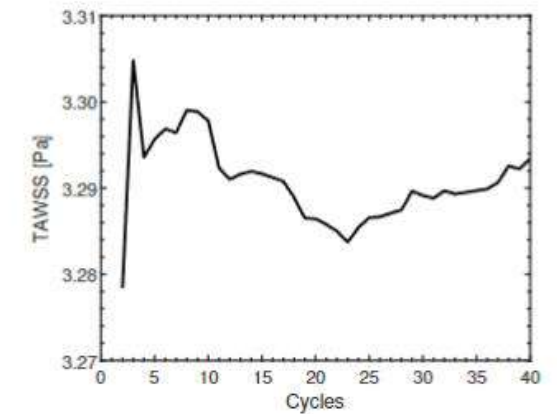
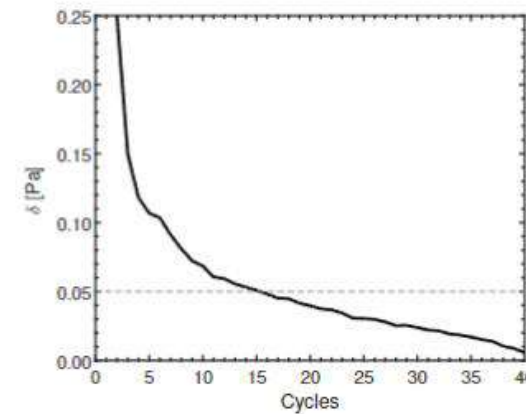


$$IF = \mu / \mu_{\infty}$$

Turbulence model	Healthy		Stenosis	
	Systole	TA	Systole	TA
Laminar	1.160	1.277	1.148	1.290
LES	1.165	1.286	1.166	1.297

Results

- ▶ Vortex structure is influenced by the turbulence model.
- ▶ Non-Newtonian viscosity has greater impact (2.9-5.0%) on wall shear stress than Large Eddy Simulation turbulence modelling (0.1-1.4%).
- ▶ Wall shear stress is underestimated when considering Newtonian viscosity by 2.9-5.0%.
- ▶ The contribution of non-Newtonian viscosity is amplified when combined with a LES model.
- ▶ Cycle-to-cycle variability can impact the results as much as the numerical model if insufficient cycles are performed.



Martinez et al., "Effect of Turbulence and Viscosity Models on Wall Shear Stress Derived Biomarkers for Aorta Simulations," *Computers in Biology and Medicine*, 167 (2023)

Future works

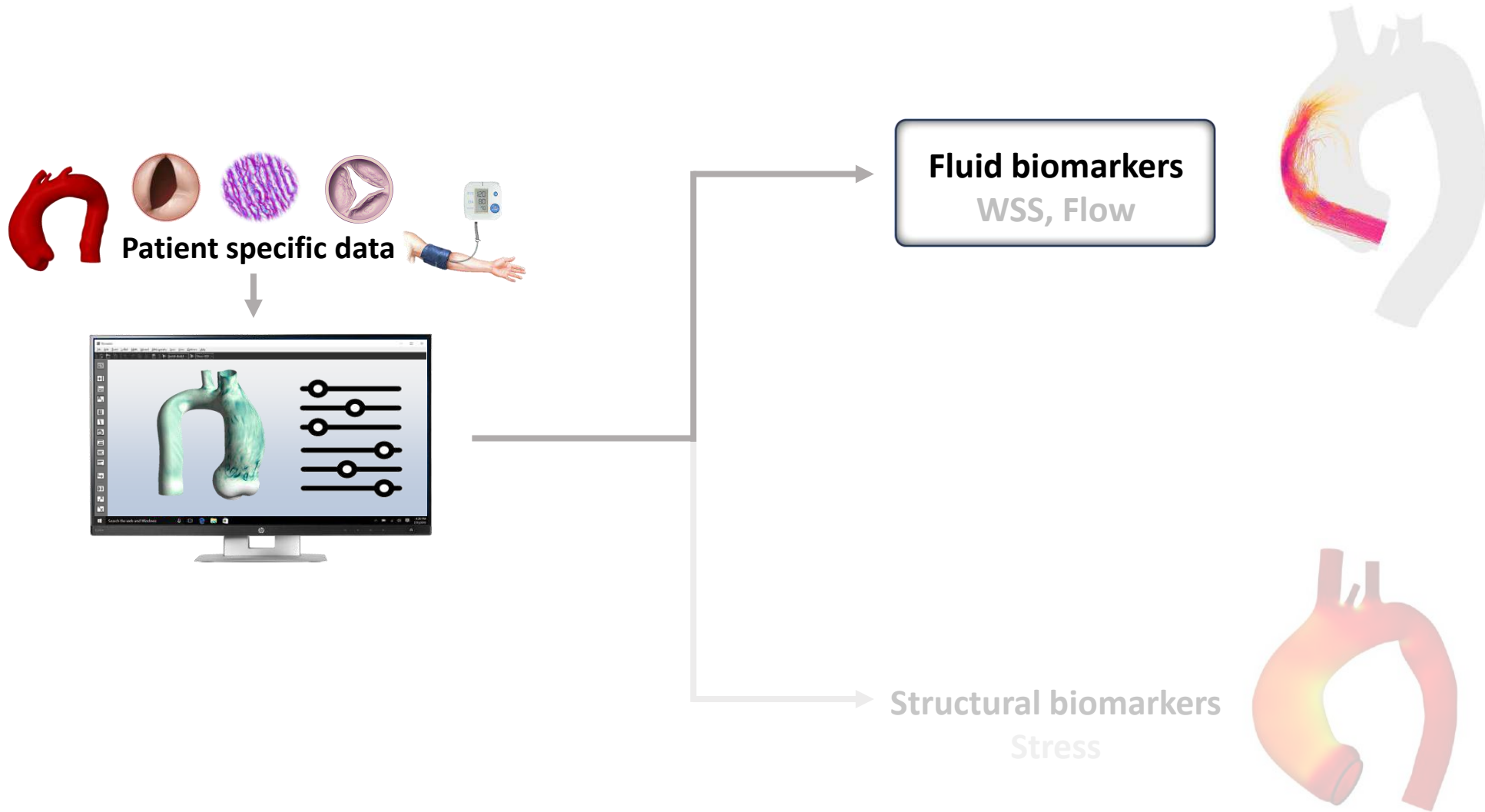
- ▶ Additional viscous models: Power law, Casson, Cross
- ▶ Realistic aortic jet shapes
- ▶ FSI effects



Section II

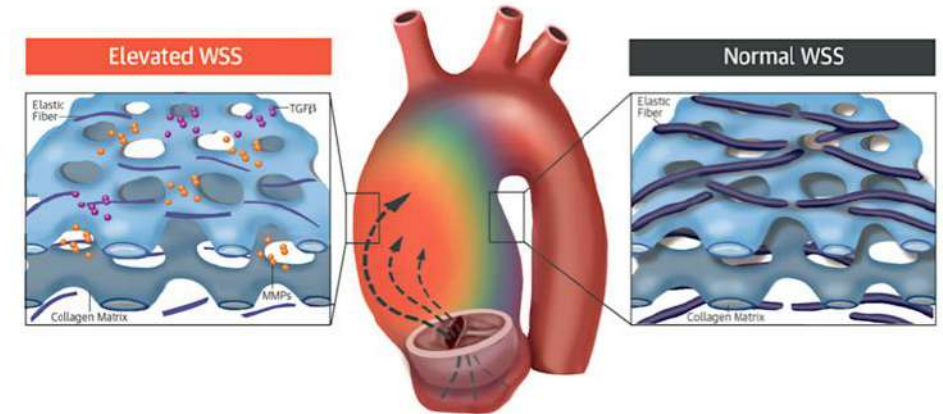
CFD biomarkers for aneurysm growth prediction

Computational tools for personalized treatment



Introduction

- ▶ Hemodynamics conditions influence the biomechanical processes in the arterial wall:
 - ▶ Endothelial damage.
 - ▶ Elastin and smooth muscle cell damage.
 - ▶ Extra cellular matrix dysregulation.
- ▶ A debate exists on whether genetic conditions or hemodynamics are responsible for the development of aneurysms.



Guzzardi et al, "Valve-Related Hemodynamics Mediate Human Bicuspid Aortopathy: Insights From Wall Shear Stress Mapping," *J. Am Coll Cardiol.* 66 (2015)

IN THIS SECTION:

The correlation between fluid biomarkers and aneurysm growth will be assessed.

Dataset



33 patients (CHU Rennes, Dijon and Toulouse)



16 Tricuspid



15 Bicuspid T1



2 Bicuspid T0



Aortic valve area and jet velocity:

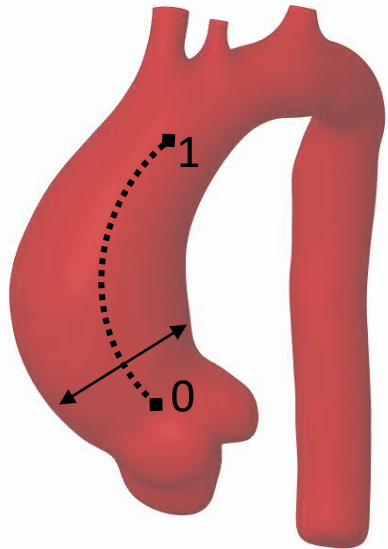
- Echocardiography: 20 patients
- MRI flow: 5 patients
- No data: 8 patients



Scans with average spacing 41 months

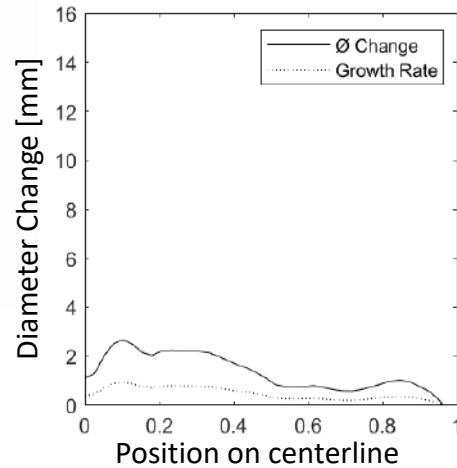
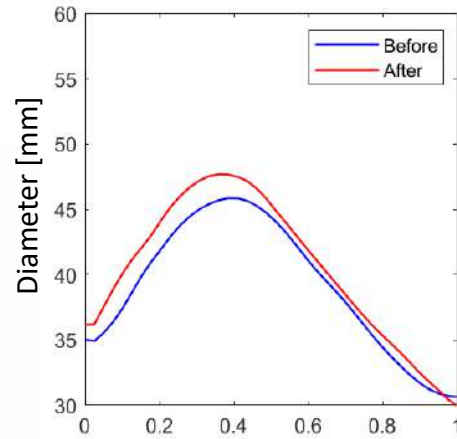
Growth analysis

Patient 1



G.R. = 0.94 mm/year

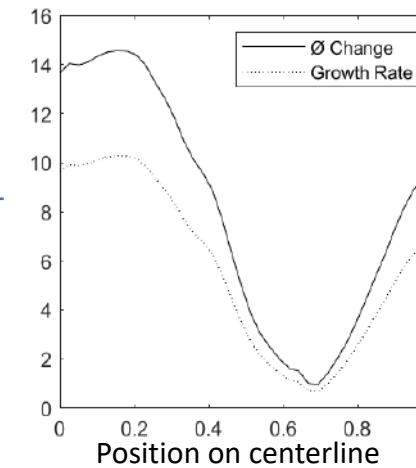
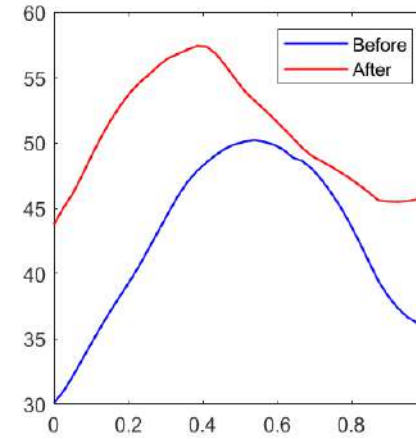
After 34 months



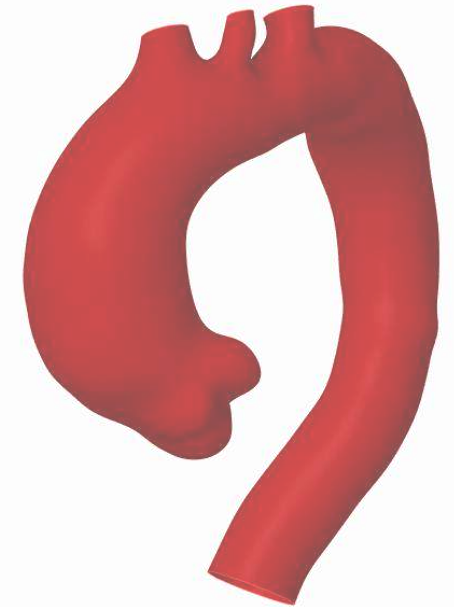
DIAMETER ALONG
THE CENTERLINE

DIAMETER CHANGE
AND
GROWTH RATE

After 17 months



Patient 2



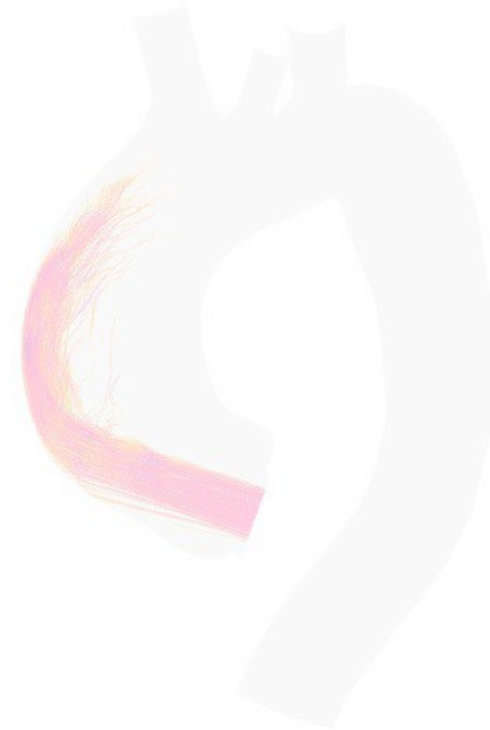
G.R. = 10.27 mm/year

Growth rate = Diameter change per year [mm/year]

Fluid Biomarkers



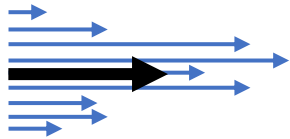
WALL SHEAR ANALYSIS



FLOW ANALYSIS

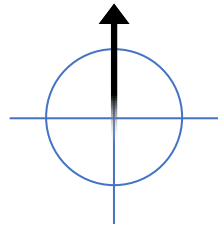
Fluid Biomarkers Wall Shear

Time-average WSS



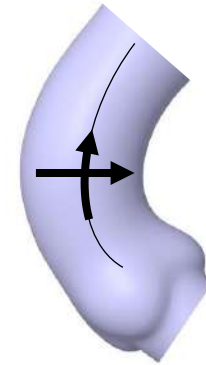
$$\text{TAWSS} = \frac{1}{T} \int_0^T |\mathbf{WSS}(t)| dt$$

Oscilating Shear Index



$$\text{OSI} = 0.5 \left(1 - \frac{\left| \int_0^T \mathbf{WSS}(t) dt \right|}{\int_0^T |\mathbf{WSS}(t)| dt} \right)$$

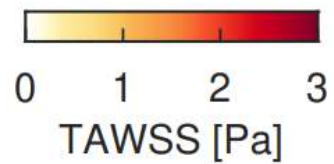
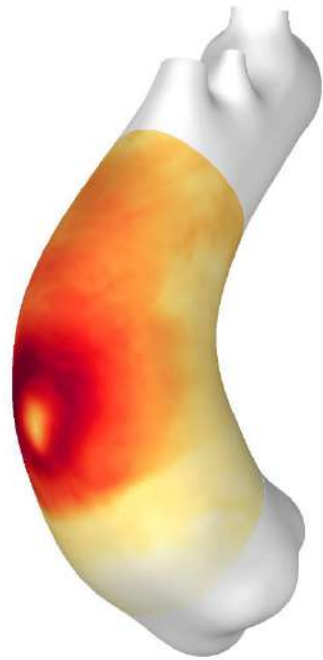
Shear Angle



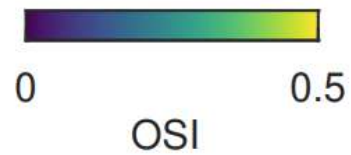
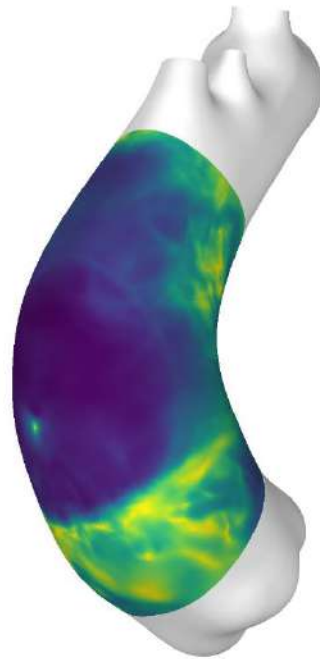
$$\text{SA} = \frac{2}{\pi} \arctan \left(\frac{\text{WSS}_{\text{Axial}}}{\text{WSS}_{\text{Circ}}} \right)$$

Fluid Biomarkers Wall Shear

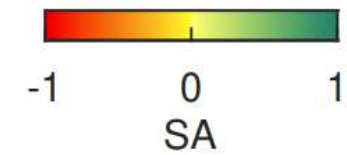
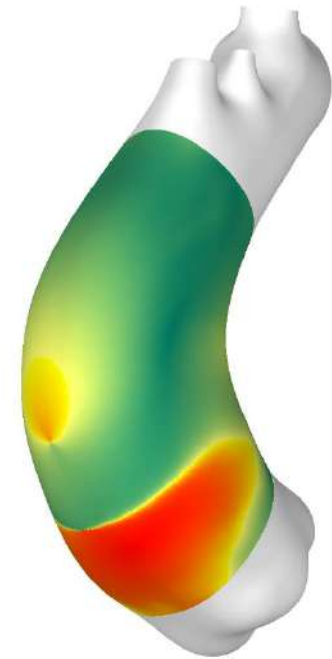
Time-average WSS



Oscilating Shear Index



Shear Angle



Fluid Biomarkers Flow



WALL SHEAR ANALYSIS



FLOW ANALYSIS

Fluid Biomarkers Flow

Flow Asymmetry:

Offset of flux centroid.

Normalized by mean radius.

$$FA = \frac{\|P_{Center} - P_{FMC}\|}{R_{mean}}$$

Angle: Between flow and plane

Flow Asymmetry - Bounded:

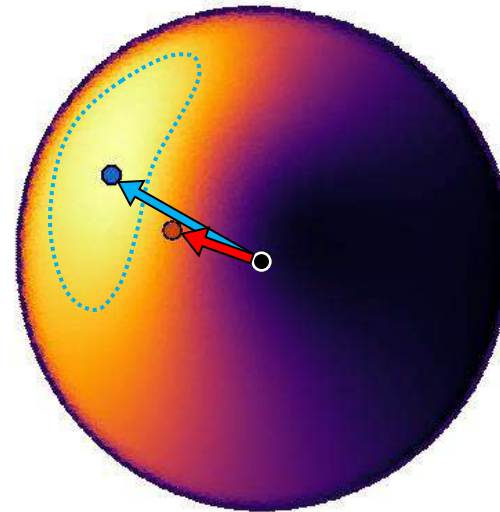
Offset of bounded fast-moving region centroid

Normalized by mean radius.

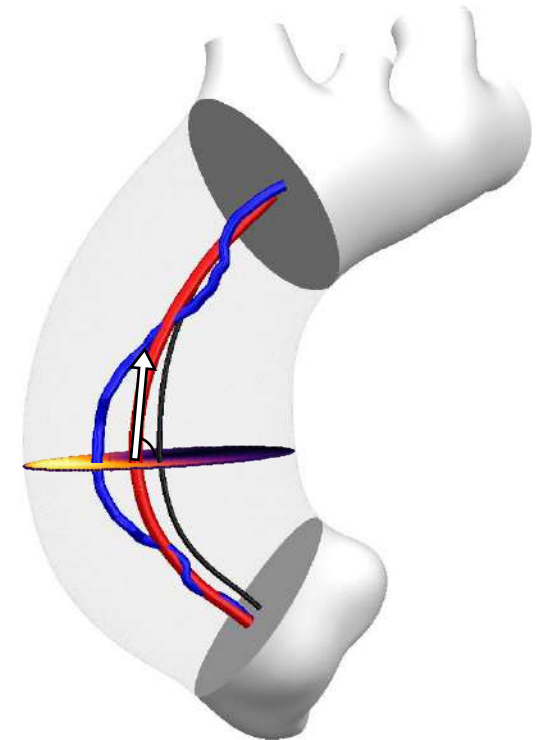
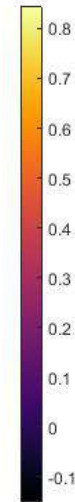
$$FA_{20\%} = \frac{\|P_{Center} - P_{FMC_{20\%}}\|}{R_{mean}}$$

Flow Dispersion:

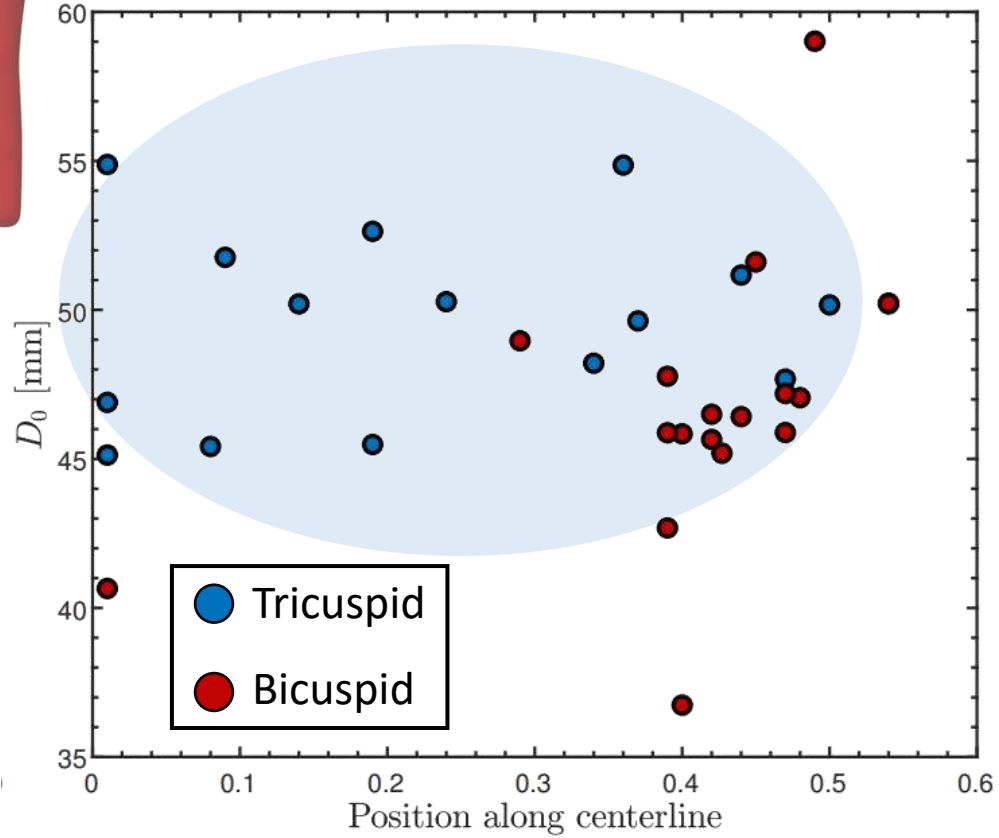
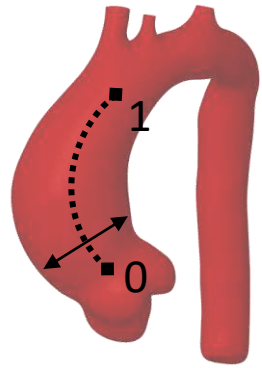
$$FD = \frac{A_{20\%}}{A_{Total}}$$



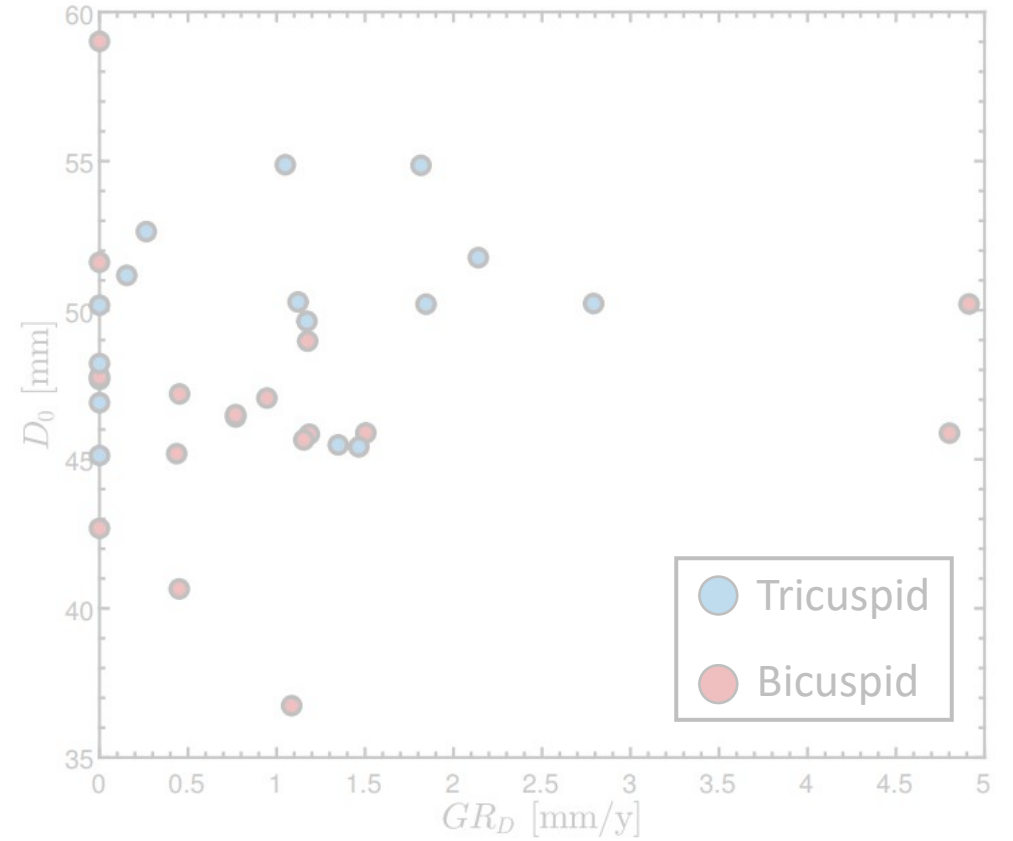
Cross-plane velocity
[m/s]



Results: Growth

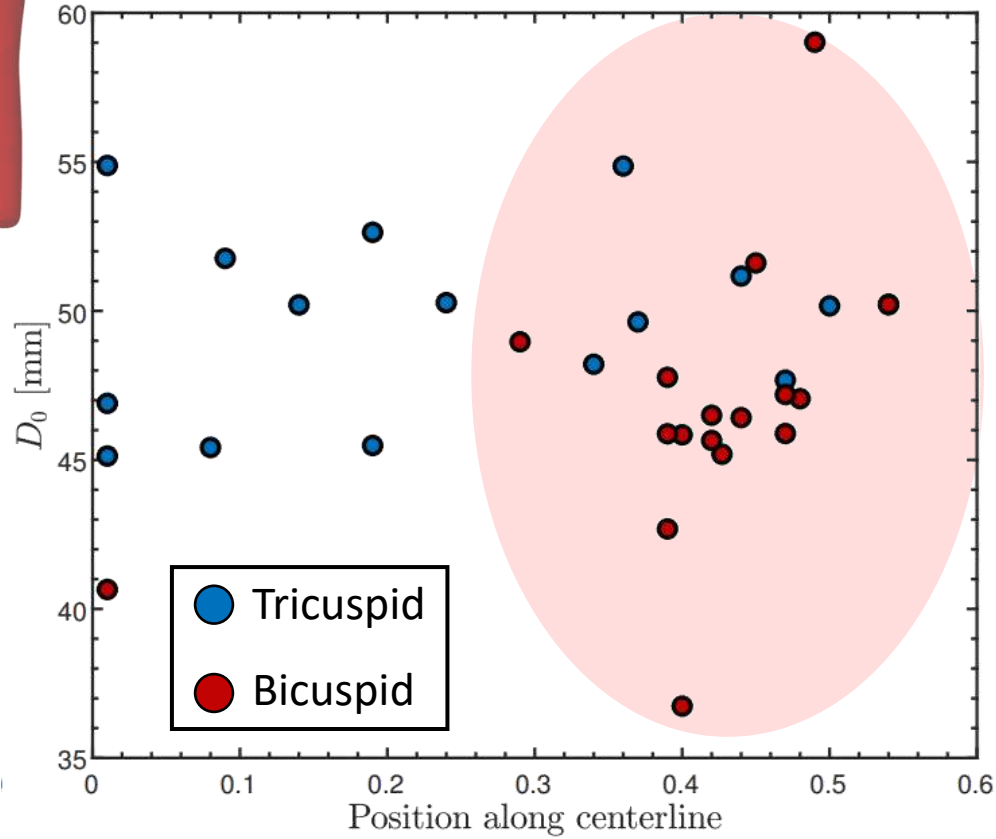
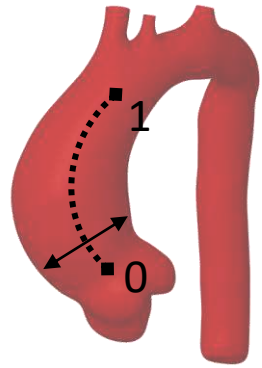


The maximum diameter was located, on average, on PC = 0.25 for TAV and on PC = 0.40 for BAV.

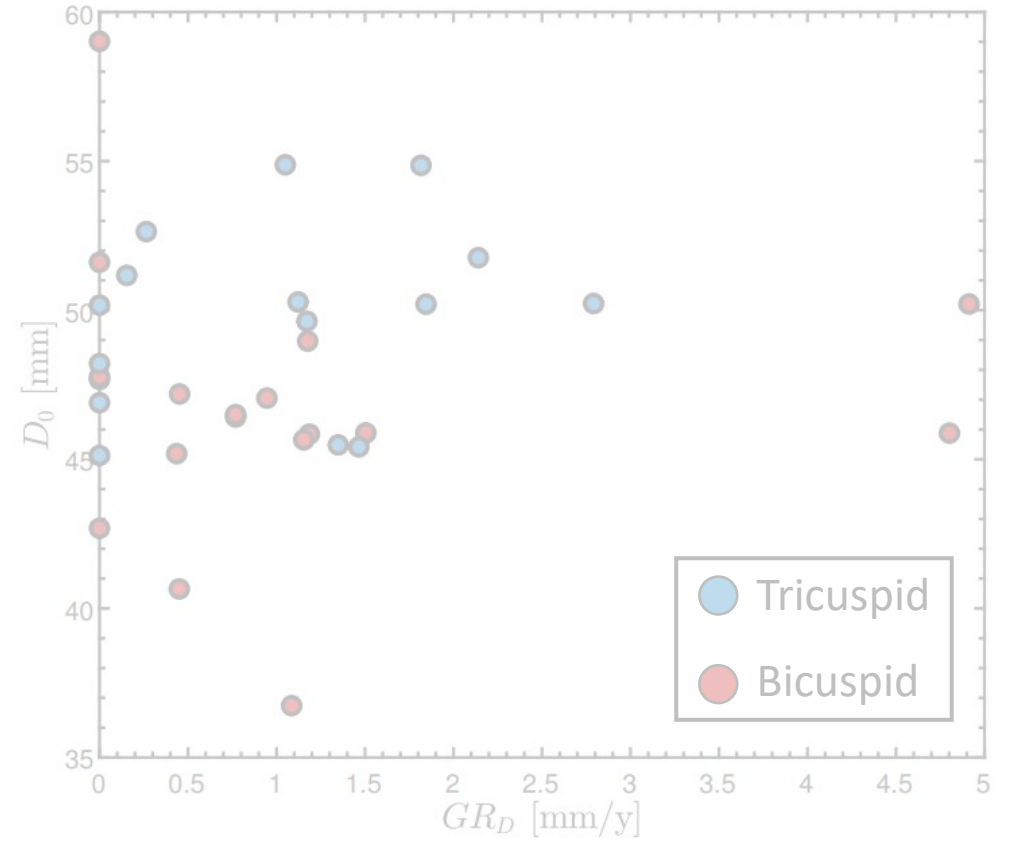


Initial diameter does not correlate with *GR* (R= 0.04)

Results: Growth

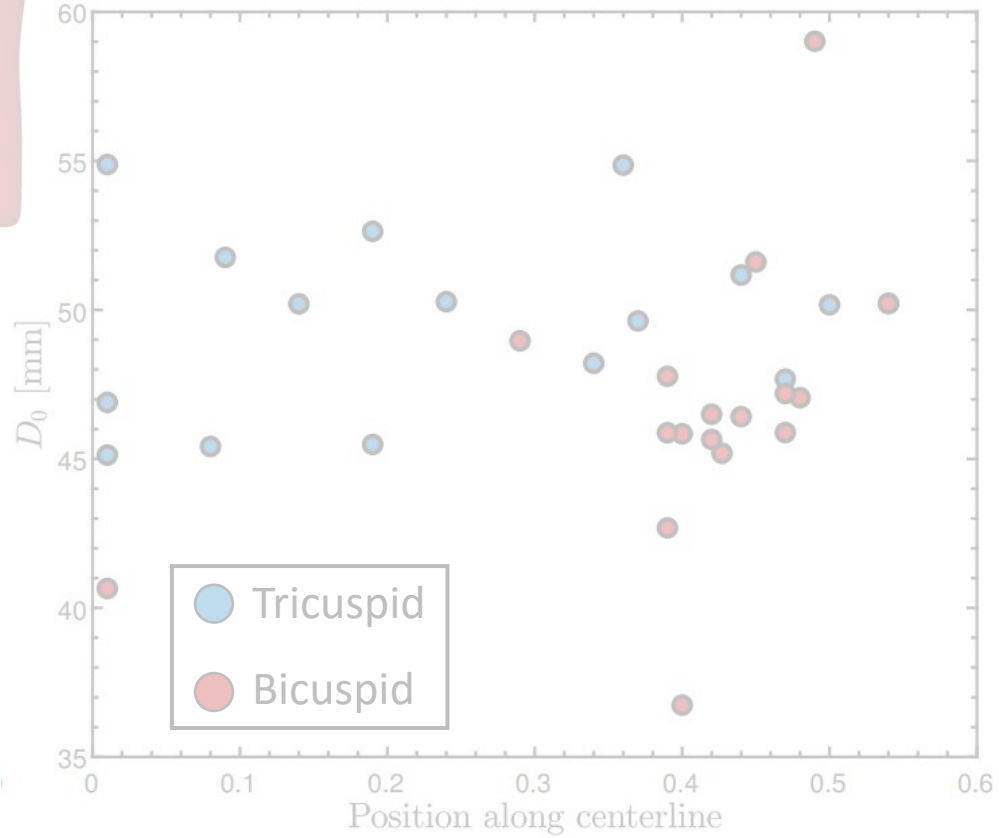
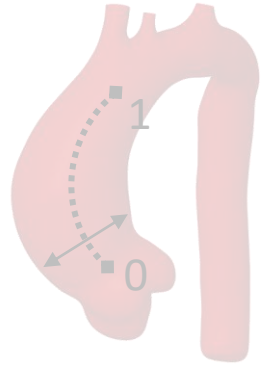


The maximum diameter was located, on average, on PC = 0.25 for TAV and on PC = 0.40 for BAV.

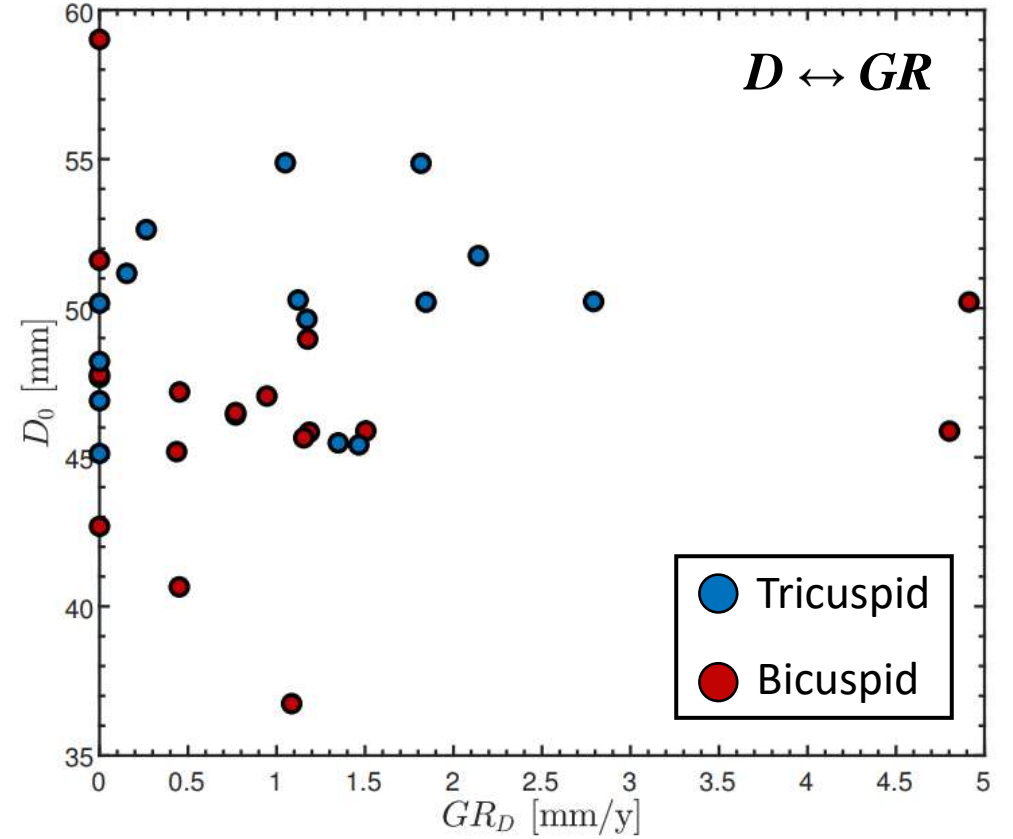


Initial diameter does not correlate with GR ($R = 0.04$)

Results: Growth



The maximum diameter was located, on average, on PC = 0.25 for TAV and on PC = 0.40 for BAV.

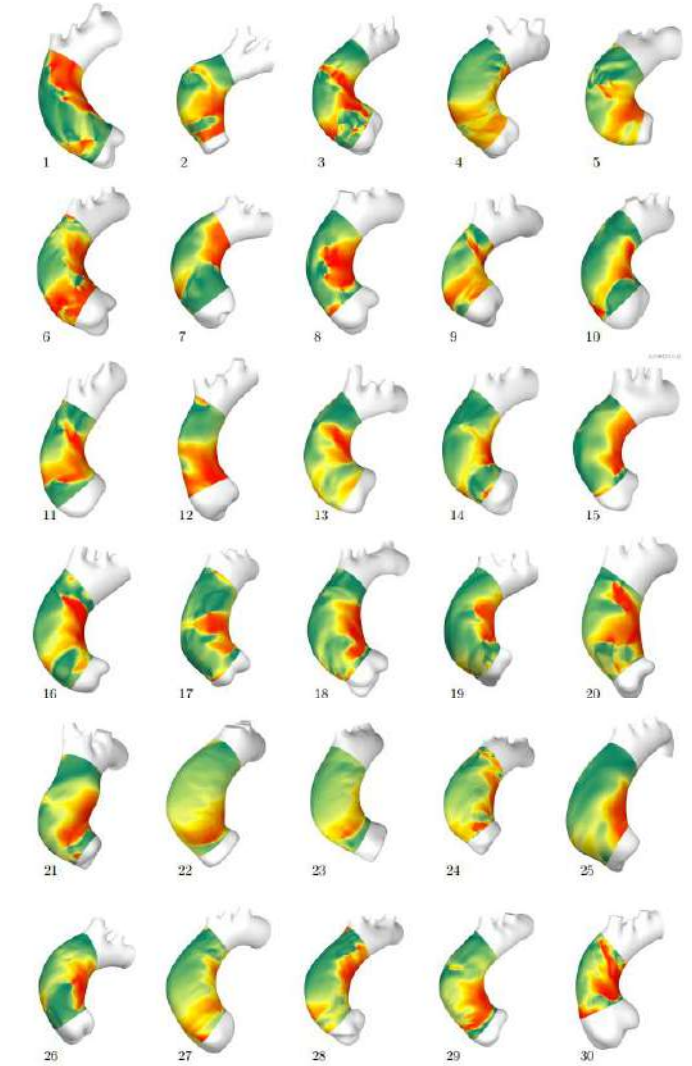
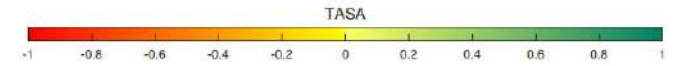
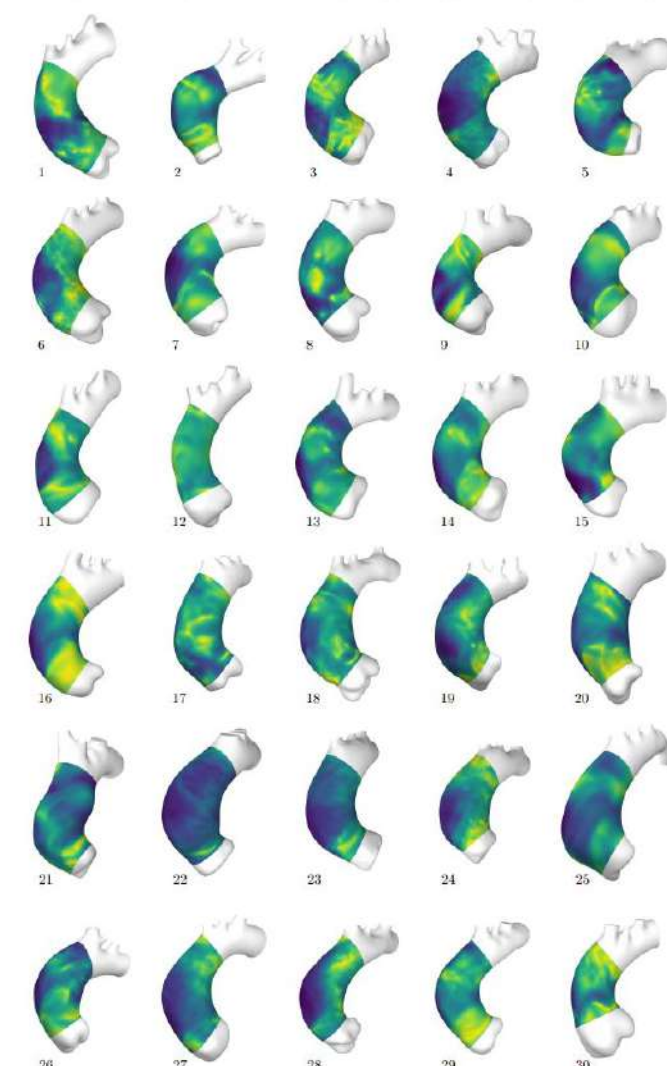
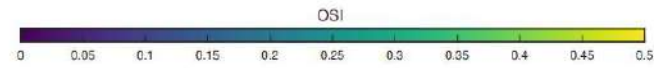
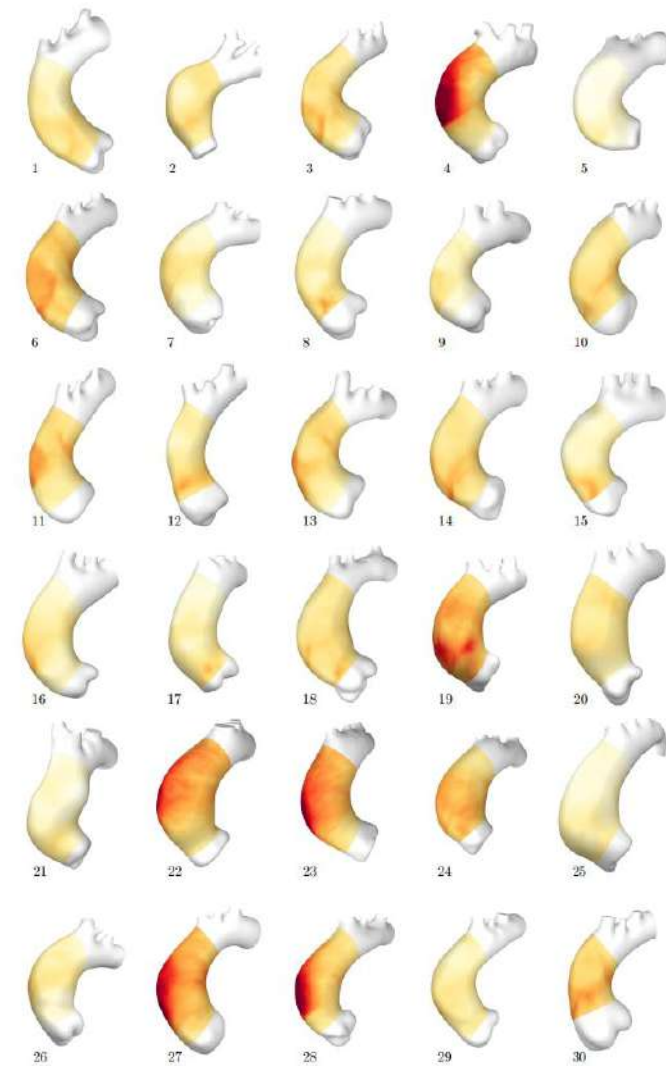


Initial diameter does not correlate with GR ($R = 0.04$)

Results: Fluid biomarkers

6 days per patient

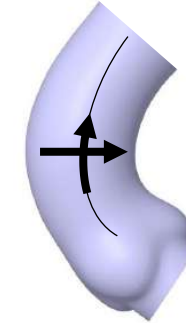
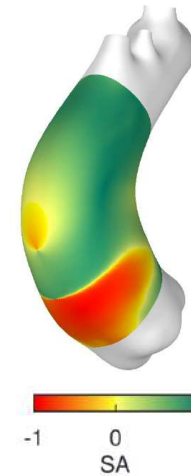
- ▶ 6 heart beats
- ▶ 16 cores
- ▶ 33 patients



Results: Correlations

PEAK SYSTOLE SHEAR ANGLE

- ▶ External wall of BAV patients.
- ▶ Weak correlation with GR_D and GR_L .
- ▶ Suggest reversed and rotating flow are linked to wall degeneration.
- ▶ Agrees with previous works:
 - ▶ FSI on Marfan syndrome patients
Pons et al., Royal Society Open Science 7 (2020)
 - ▶ MRI flow on BAV patients
Minderhoud et al., European Heart Journal – Cardiovascular Imaging 23 (2022)
- ▶ Only 17 BAV patients → Statistical relevance is debatable.
- ▶ Largest CFD study on aneurysm growth up to date.

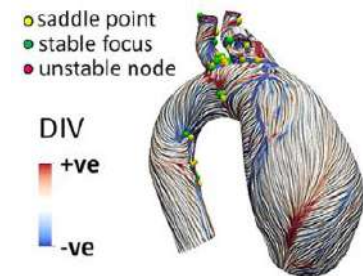
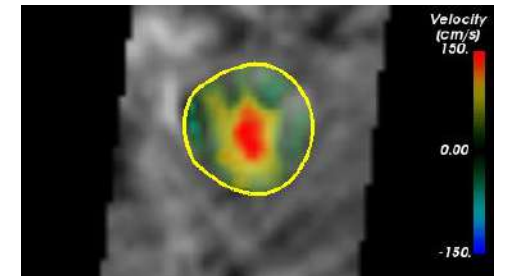
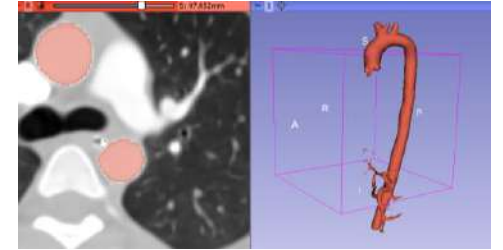


$$SA = \frac{2}{\pi} \arctan \left(\frac{WSS_{Axial}}{WSS_{Circ}} \right)$$

Biomarker	Measure	TAV				BAV			
		GR_D		GR_L		GR_D		GR_L	
		R	p	R	p	R	p	R	p
TAWSS	Max	-0.223	0.407	-0.274	0.304	-0.160	0.541	-0.256	0.321
	Mean	-0.054	0.843	-0.190	0.480	-0.128	0.623	-0.209	0.421
PSWSS	Max	-0.132	0.626	-0.162	0.549	-0.053	0.841	-0.148	0.570
	Mean	-0.178	0.510	-0.282	0.291	-0.095	0.717	-0.213	0.411
OSI	Mean	-0.030	0.911	0.108	0.692	-0.089	0.734	0.002	0.995
SA	TA-Mean	0.061	0.823	-0.048	0.860	0.255	0.324	0.274	0.287
	PS-Mean	0.004	0.987	-0.048	0.859	-0.482	0.050	-0.481	0.051
RFR	TA	0.034	0.899	0.073	0.787	-0.266	0.303	-0.306	0.232
	PS	0.048	0.859	0.072	0.792	0.243	0.347	0.275	0.286

Future Works

- ▶ **Larger time window**
Reduce the error in the growth rate measurements.
Follow the evolution during the initial phase.
- ▶ **MRI 4D calibrated aortic jet**
The spatio-temporal velocity profile of the aortic jet will severely determine the flow structure throughout the cardiac cycle, hence, the biomarkers.
- ▶ **Topological WSS skeleton analysis**
Evaluated the topological shear variation index (TSVI) and fixed-point relative residence time (RTV).

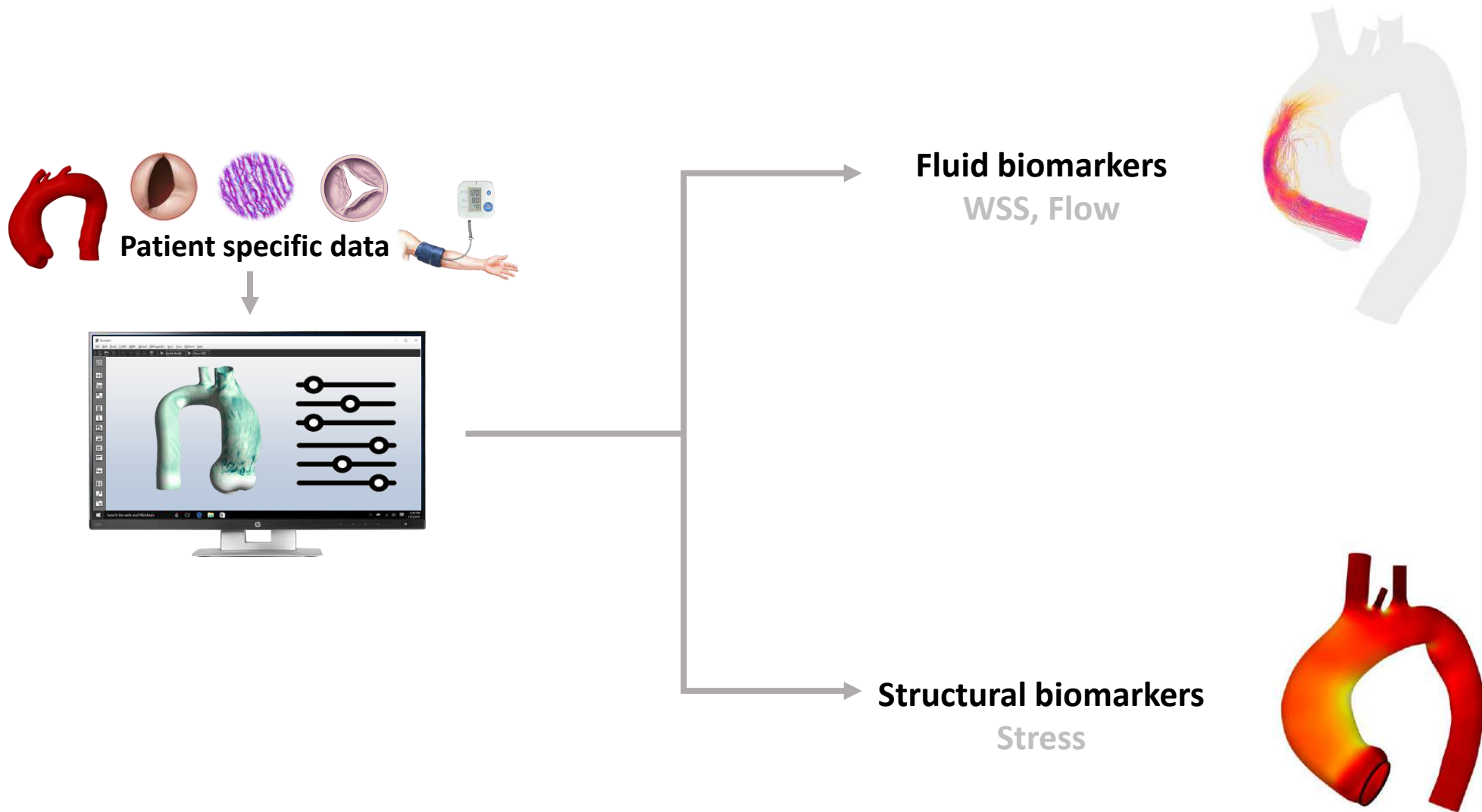


A microscopic view of red blood cells, showing their characteristic biconcave disc shape and reddish color. The cells are scattered across the field of view, with some in sharp focus and others blurred in the background.

Section III

Patient-specific FSI models

Computational tools for personalized treatment

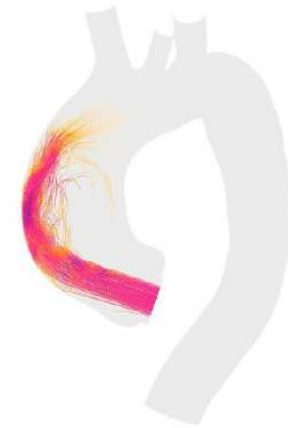


Computational tools for personalized treatment

Personalized hemodynamic conditions

- ▶ Aortic jet derived from MRI 4D flow
- ▶ Windkessel outlets calibrated with patient's data

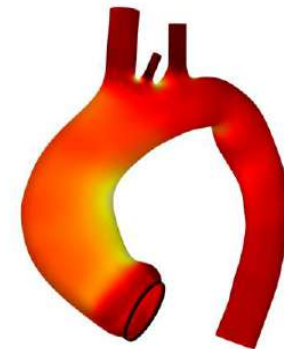
Fluid biomarkers
WSS, Flow



Personalized aorta wall

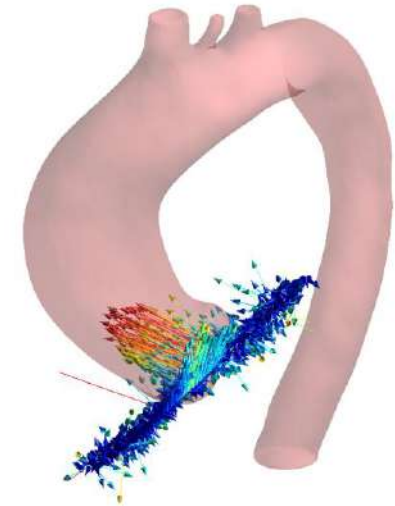
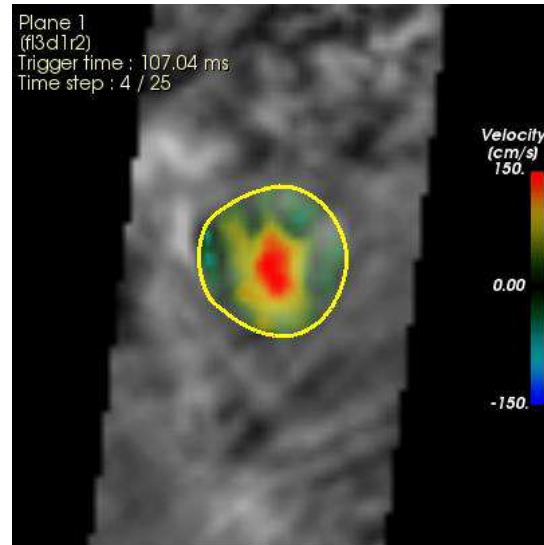
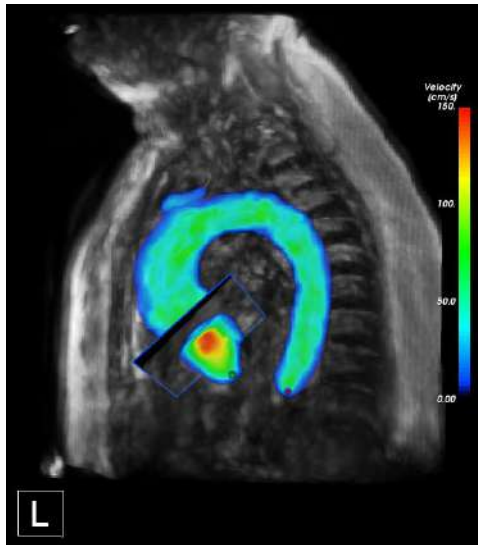
- ▶ Thickness
- ▶ Elasticity

Structural biomarkers
Stress



Methods: Aortic jet

MRI 4D Flow



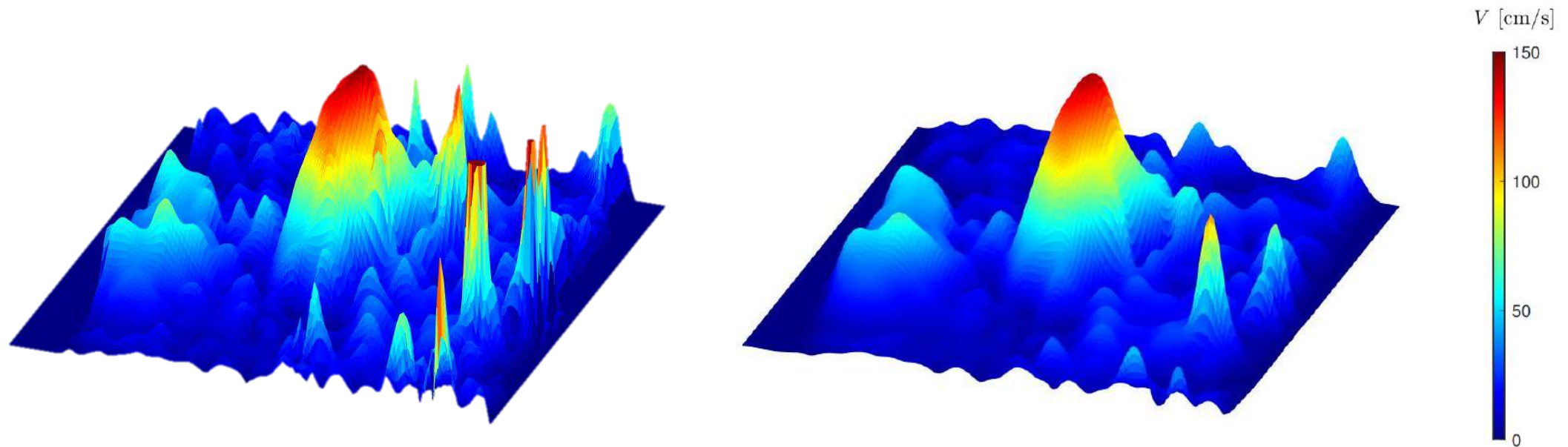
Velocity extraction on aortic valve plane

Transfer onto the fluid model

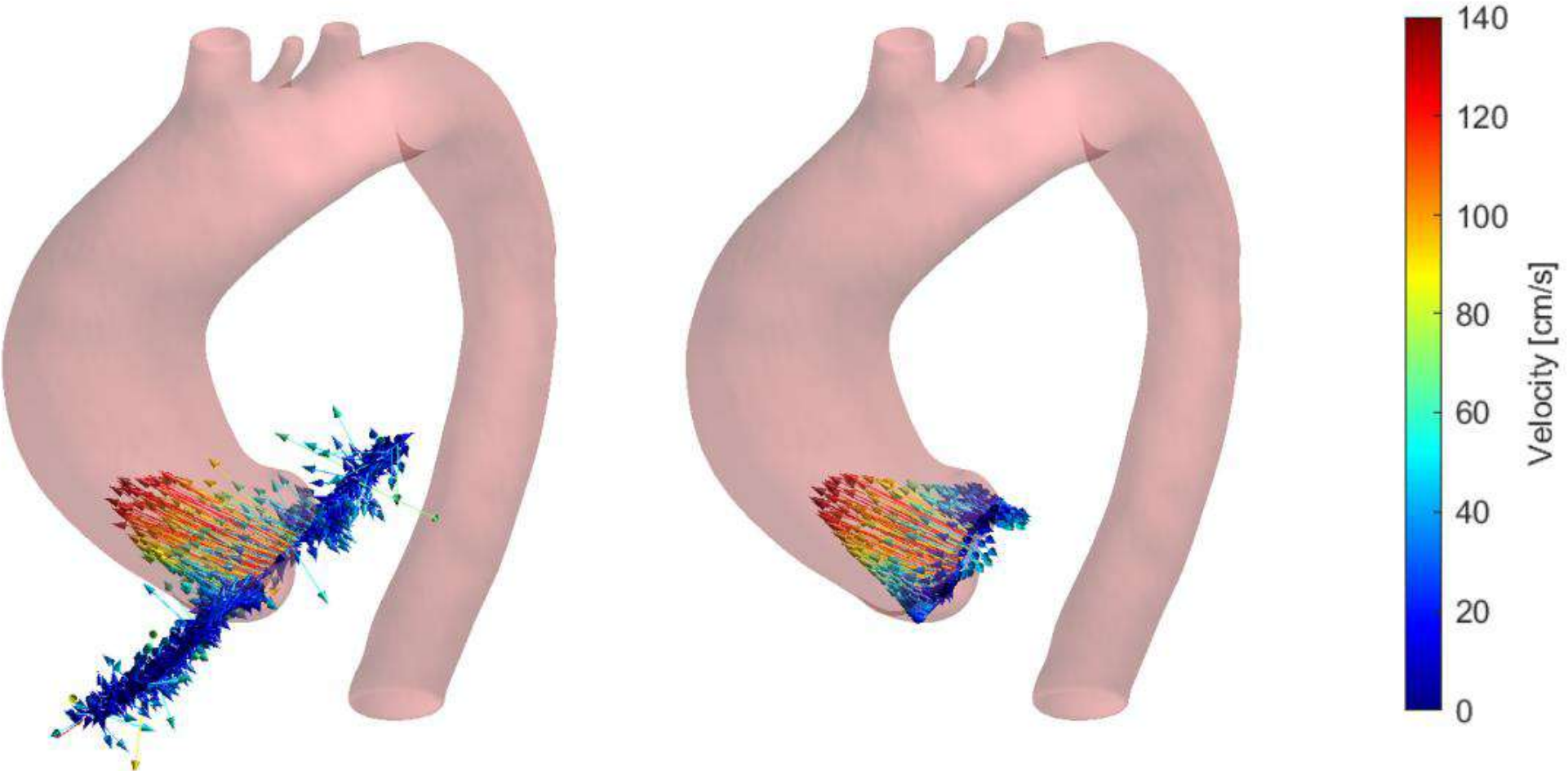
Methods: Aortic jet

Resampling and filtering:

- ▶ Finer grid (x3) using modified Akima interpolation: reduced undulations and over-flattening.
- ▶ Gaussian 2-D filter was applied to smooth each of the three velocity components. Smoothing kernel with standard deviation 2.5.



Methods: Aortic jet



Methods: Windkessel

DATA

Measure	Value	Unit
Q_{max}	456.2	ml/s
Q_{min}	15.3	ml/s
Q_{mean}	6.89	l/min
Q_{DA}	3.48	l/min
P_{Sys}	60	mmHg
P_{Dias}	0.0	mmHg
Δt	0.1	s
A_{BT}	185.2	mm ²
A_{LCC}	20.4	mm ²
A_{LS}	67.3	mm ²



METHOD

$$R_T = \frac{P_{mean}}{Q_{mean}},$$

$$R_i = R_T / f_i,$$

$$C_T = \frac{Q_{max} - Q_{min}}{P_{Sys} - P_{Dias}} \Delta t,$$

$$C_T^* = C_T - C_{As}^{3D},$$

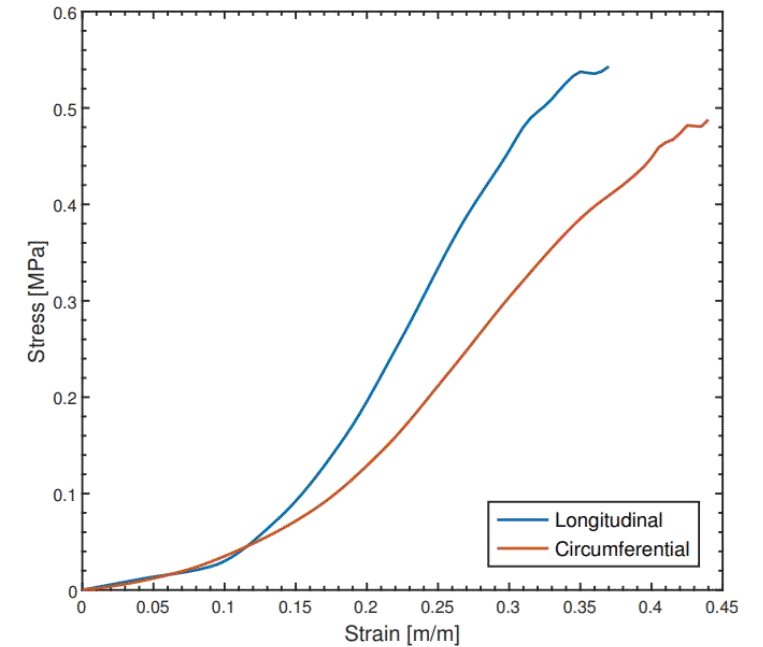
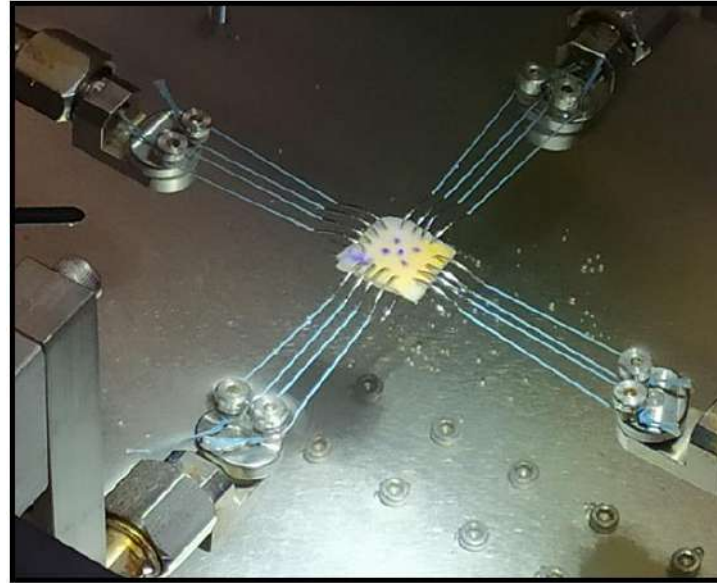
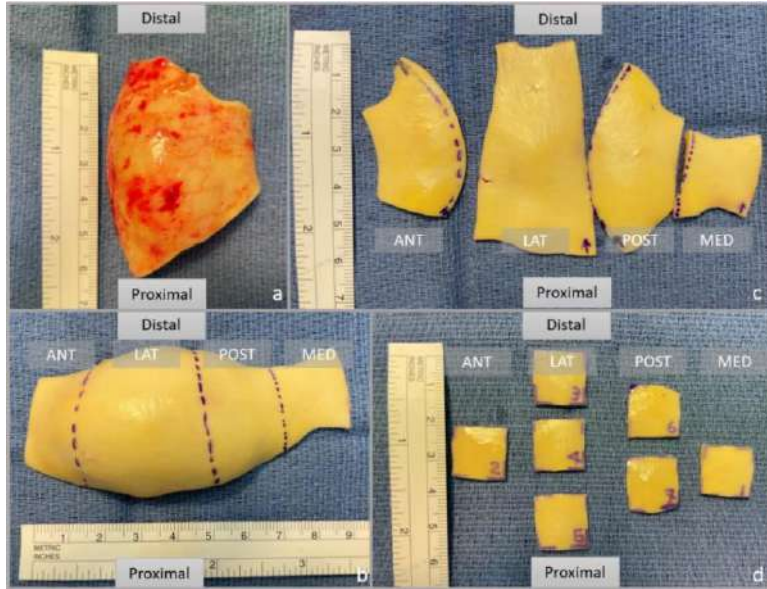
$$C_i = f_i C_T^* \frac{R_i}{R_{d_i}} = C_T^* \frac{R_T}{R_{d_i}}.$$

RESULTS

Component	Value
R_{pBT}	3.858×10^6
R_{dBT}	6.504×10^7
C_{BT}	1.587×10^{-9}
R_{pLCC}	3.569×10^7
R_{dLCC}	6.016×10^8
C_{LCC}	1.715×10^{-10}
R_{pLS}	1.065×10^7
R_{dLS}	1.796×10^8
C_{LS}	5.746×10^{-10}
R_{pDA}	2.575×10^6
R_{dDA}	4.340×10^7
C_{DA}^*	9.407×10^{-10}

Methods: Aortic wall - Clinical data

4 sections: Anterior, lateral, posterior and medial



Equi-biaxial tensile test performed in the University Hospital of Dijon.

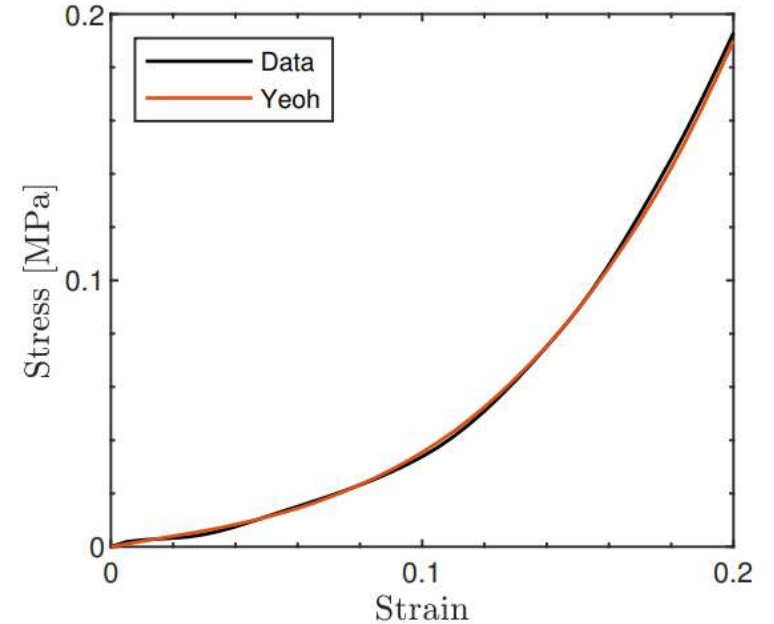
S. Lin, "Biomechanics of human ascending aorta and aneurysm rupture risk assessment", PhD Thesis, 2021.

Methods: Aortic wall - Hyperelastic material

Ascending aorta: Third order Yeoh material model.

$$W = \sum_{i=1}^3 C_{i0} (\bar{I}_1 - 3)^i.$$

The model coefficients for each quadrant were obtained after performing a curve fitting via minimization of normalized error of the circumferential strain-stress curves.



Supra-aortic vessels and DA: Second order Yeoh material model derived from estimated pulse wave velocity (PWV).

$$PWV = \frac{\alpha}{(2 \times 10^3 r_v)^\beta} \quad E_{inc} = \frac{2r_v \rho}{T_v} PWV^2$$

Methods: Aortic wall - Model definition

Spatially varying material properties

Ascending aorta: 2 node interpolation

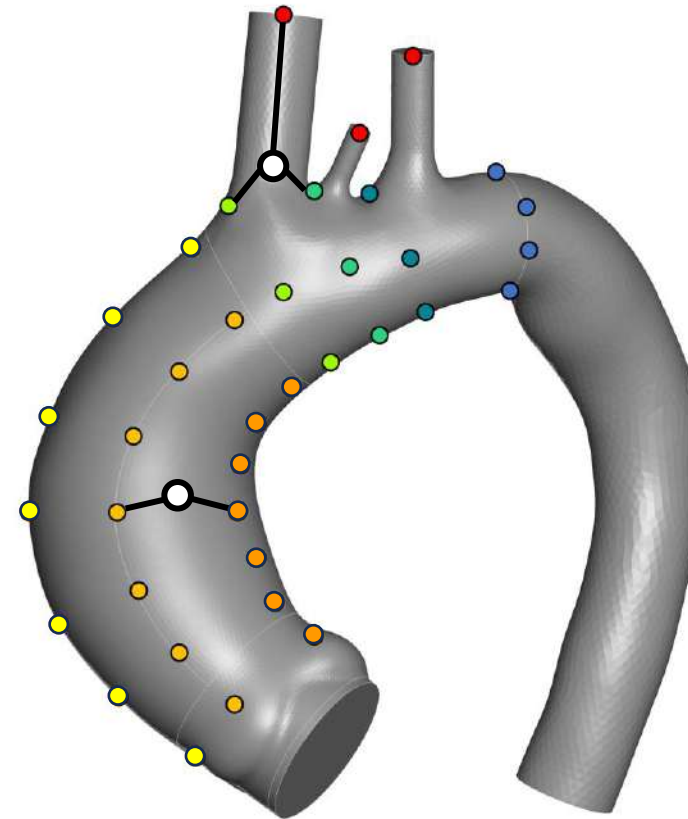
$$T_n = T_{s1} \frac{D_{n,s1}}{D_{n,s1} + D_{n,s2}} + T_{s2} \frac{D_{n,s2}}{D_{n,s1} + D_{n,s2}}$$

Aortic arch: 3 node interpolation

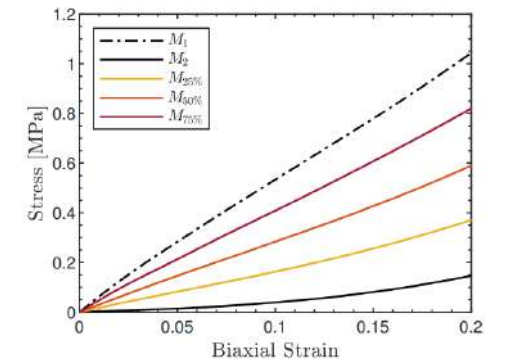
$$D_{n,v}^{\text{mod}} = D_{n,v}^* \frac{D_{\text{Lim}}}{D_{\text{Lim}} - D_{n,v}^*}$$

$$T_n = T_n^* \frac{D_{n,s}^{\text{Min}}}{D_{n,s}^{\text{Min}} + D_{n,v}^{\text{mod}}} + T_v \frac{D_{n,v}^{\text{mod}}}{D_{n,s}^{\text{Min}} + D_{n,v}^{\text{mod}}}$$

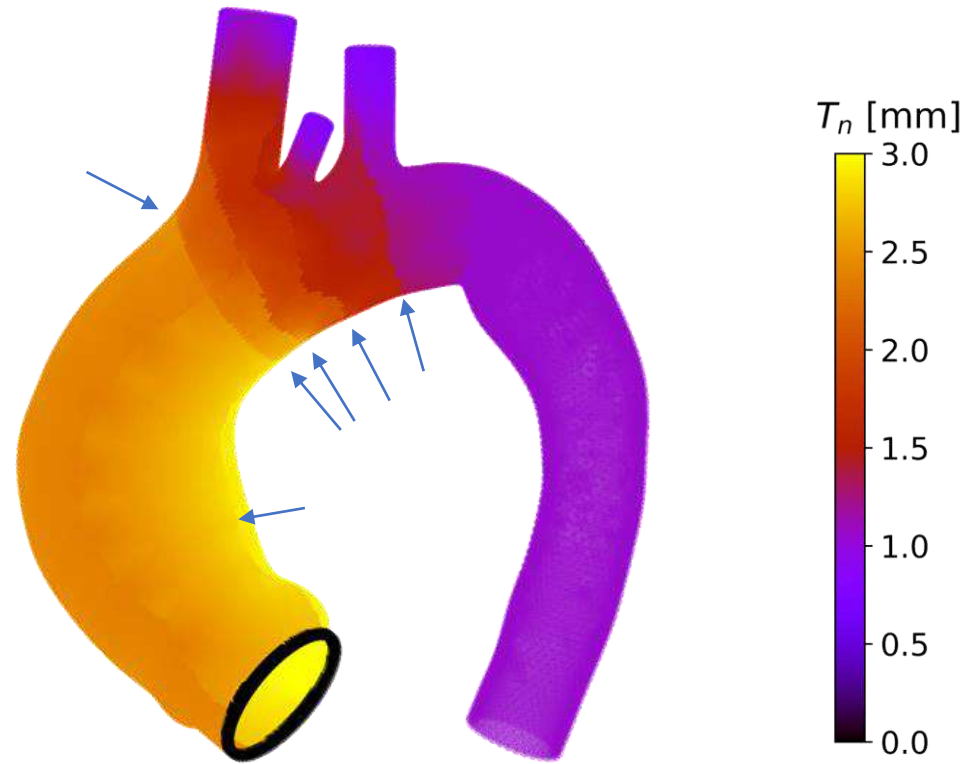
DA: Constant properties



- Ascending aorta
- Arch set 1
- Arch set 2
- Arch set 3
- Descending aorta
- Supra-aortic vessels

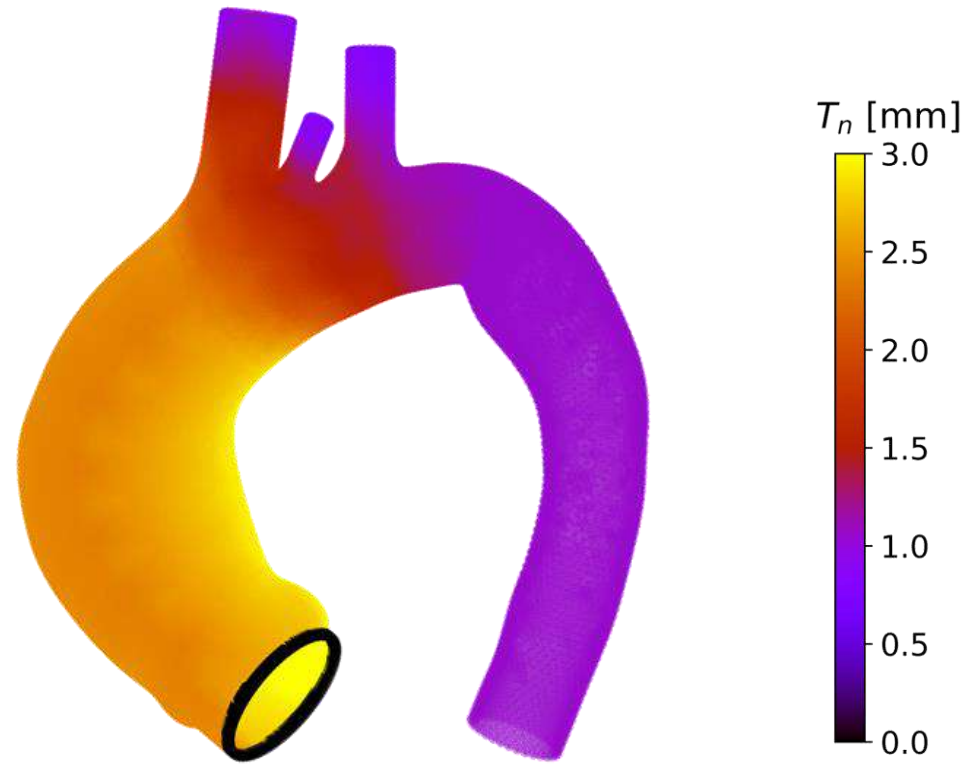


Methods: Aortic wall - Model definition



Initial

Methods: Aortic wall - Model definition



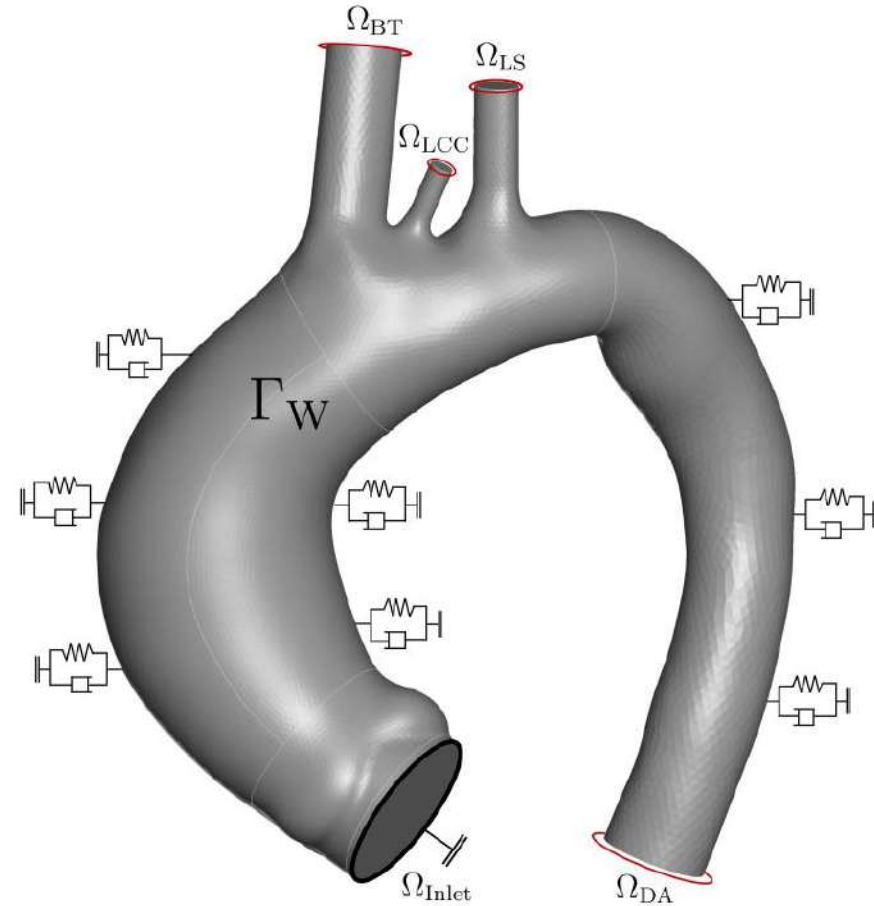
Smooth

Methods: Aortic wall - Boundary conditions

- ▶ Radial displacement on outlets
- ▶ Viscoelastic support on wall

$$K_{n_j} = (K_{\text{Soft}} + W_d W_j K_{\text{Spine}}) A_n e_{n_j},$$

Coefficient	Value
K_{Soft}	1.5×10^4 Pa/m
K_{Spine}	10^6 Pa/m
W_d	0.53
W_x	0.60
W_y	0.02
W_z	0.04

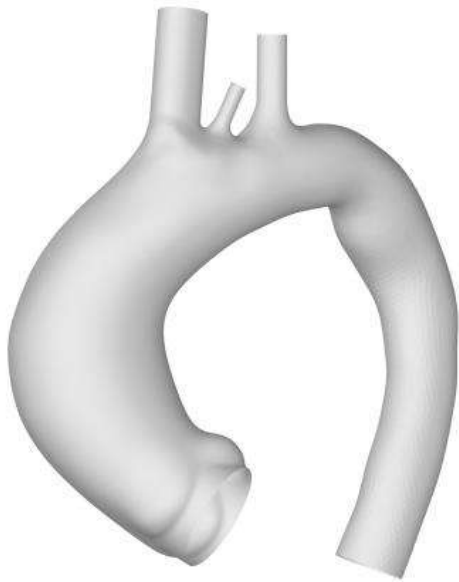


Geronzi et al., "Calibration of the Mechanical Boundary Conditions for a Patient-Specific Thoracic Aorta Model Including the Heart Motion Effect," *IEEE Trans Biomed Eng.* 70-11 (2023)

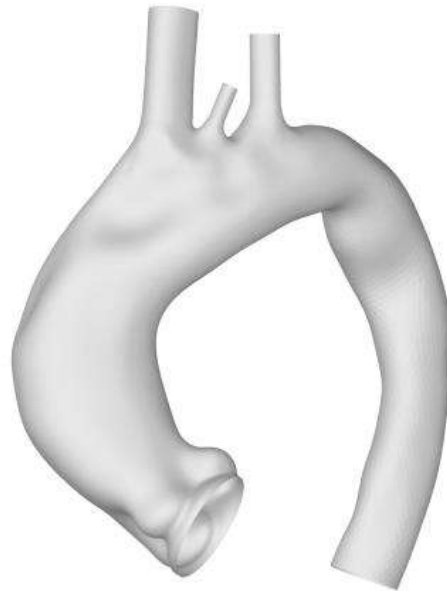
Methods: Aortic wall - Zero pressure

Augmented Sellier's Inverse Method

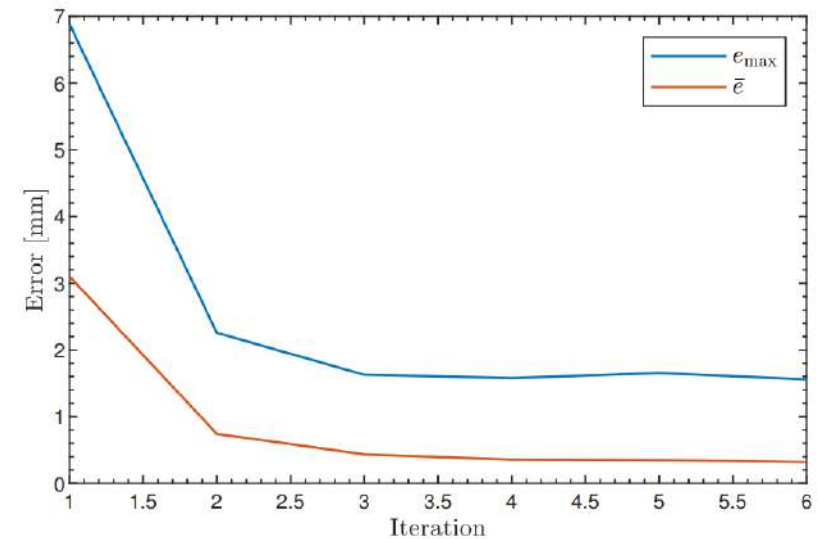
- ▶ Inverse problem: loads and final deformation are known, initial geometry is to be computed.
- ▶ The zero-stress state will be approximated by the zero pressure state.



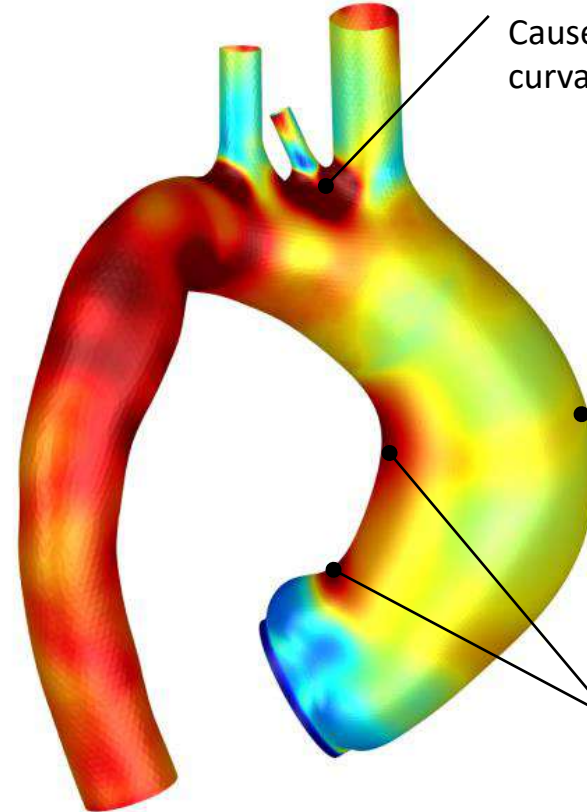
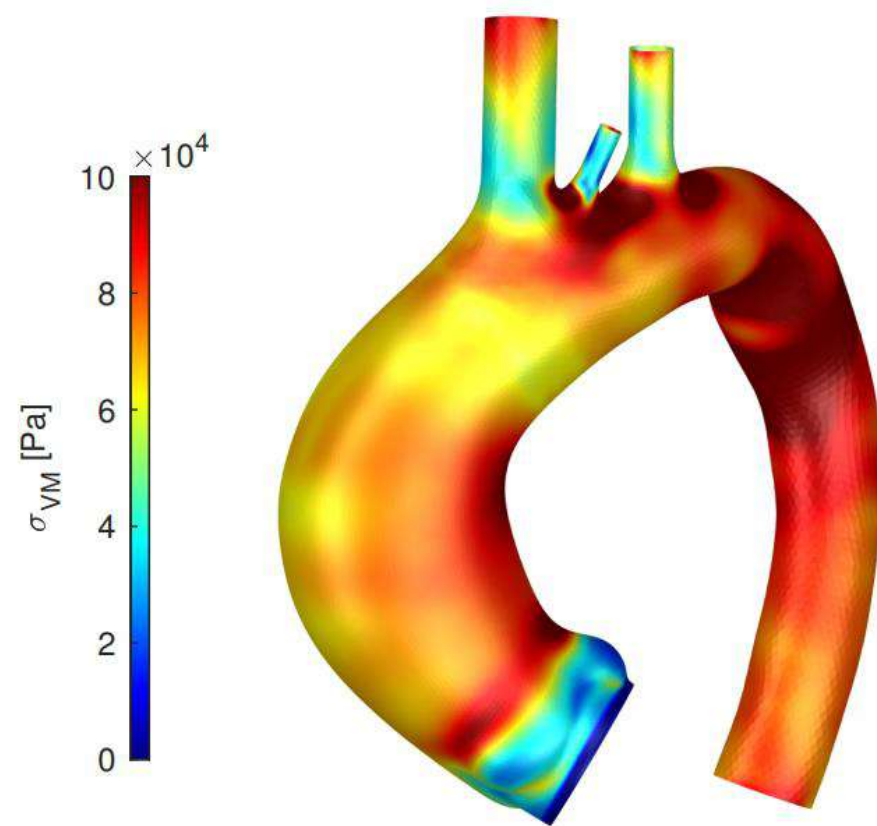
Reference



Zero pressure



Results: Stress



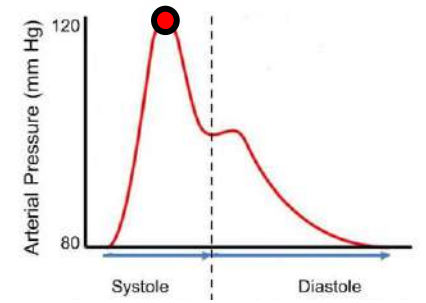
Arch: 345 kPa

Caused by high, unrealistic curvature and shell formulation

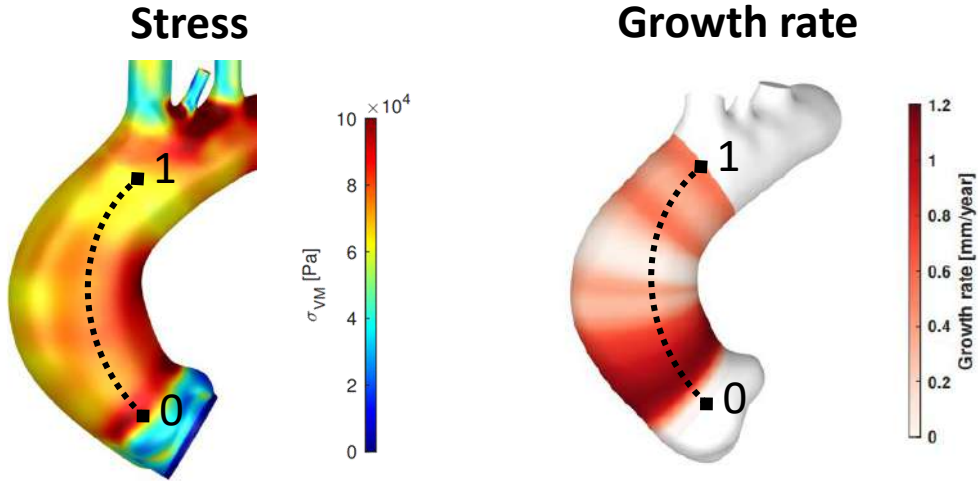
External wall: 50-80 kPa

Internal wall: 100-105 kPa

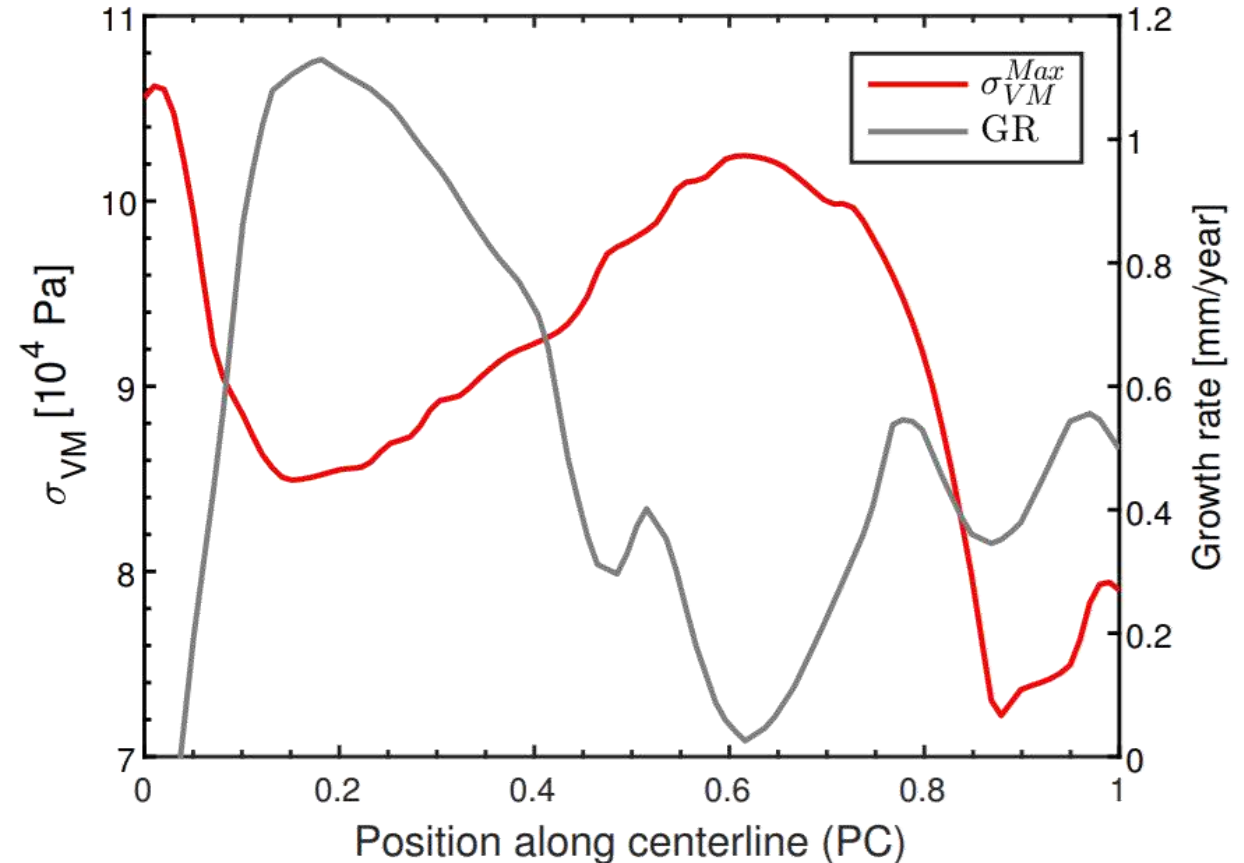
42% of maximum yield strength



Results: Stress - Growth



- ▶ No evidence of a correlation between stress and aneurysm growth.
- ▶ Locations with highest stress concentration show null growth.



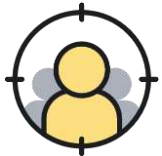
Conclusions



Clinical outcomes: one patient only, it is not possible to hypothesise on the relationship between growth and stress.



A large cohort should be analysed, considering both healthy, stable and dilating aneurysms.

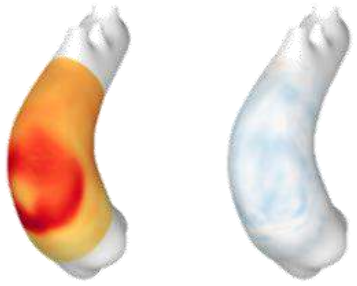


A model combining patient specific hemodynamics and aorta wall has been presented. Further improvements will enable an accurate estimation of risk of rupture.

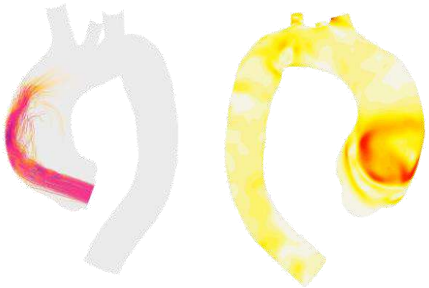
A microscopic view of red blood cells (erythrocytes) in a blood smear. The cells are biconcave discs, appearing as reddish-orange discs with a lighter center. They are scattered across the field of view, with some in sharp focus and others blurred. The background is a light, slightly hazy pinkish-white.

Final conclusions

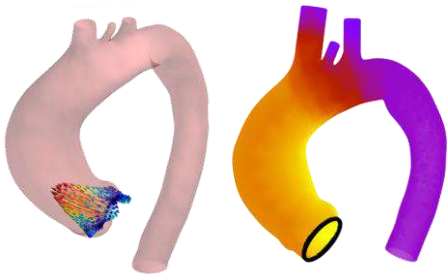
Final Conclusions



- ▶ Non-Newtonian viscosity is necessary.
- ▶ LES is optional, but computational requirement is negligible.



- ▶ Aneurysm growth could be related to:
 - ▶ BAV: Peak systole shear angle.
- ▶ Larger cohort with MRI flow data is needed.



- ▶ Hemodynamic personalization requires MRI 4D flow data.
- ▶ Aorta wall definition requires spatially varying thickness and elastic properties.
- ▶ Accurate risk of rupture estimation requires high fidelity models.



The work has received funding from the European Union's Horizon 2020 research and innovation programme under the Marie Skłodowska-Curie grant agreement No 859836, MeDiTATe: "The Medical Digital Twin for Aneurysm Prevention and Treatment".